

FUELING THE AGN

F. COMBES

*Observatoire de Paris, DEMIRM, 61 Av. de l'Observatoire, F-75 014, Paris,
FRANCE*

E-mail: francoise.combes@obspm.fr

Active Galactic Nuclei are fueled from material (gas or stars) that are in general far away from the gravitational influence of the central black hole, the engine thought to be responsible for their activity. The required material has a lot of angular momentum, that is a priori quite difficult to evacuate. The various dynamical mechanisms that may play a role in this game are reviewed, including $m = 2$ perturbations (bars and spirals), $m = 1$ perturbations (spirals, warps, lopsidedness), and tidal interactions between galaxies and mergers. In the latest stages of the merger, a binary black hole could be formed, and its influence on the dynamics and fueling is discussed. Starbursts are often associated with AGN, and the nature of their particular connection, and their role in the nuclear fueling is described. Evolution of the fueling efficiency with redshift is addressed.

1 Introduction

Some galaxies are dubbed “active”, which means that they radiate much more energy than can be sustained by a normal evolution rate, or average gas consumption rate, given their size and gas reservoir mass. Their activity could be due to a starburst, or to a material-accreting compact nucleus. Both are often related or simultaneous. The activity has a short duration with respect to the galaxy life-time, but can be recurrent. A key issue is to understand the mechanisms that trigger the activity, and how a large amount of material can be funneled to the central regions, to fuel this activity.

A first possibility is provided by the dense star clusters that are present near the nucleus. These nearby stars can provide gas fuel to the nucleus through their mass loss rates, or even the tidal disruption of stars can liberate their whole gas mass. We will present and discuss the various physical phenomena involved, and their respective time-scales in section 2: only those stars that have low angular momentum orbits are available to fuel the activity, but these can be replenished through dynamical diffusion when depleted. A bigger problem arises when the nearby stars are not numerous enough to sustain the activity: mass has then to come from the whole galaxy in a short time-scale, and this rises the problem of angular momentum transfer, that must involve internal or externally-triggerred gravitational instabilities. Note that the mass fueling can occur in two steps: a first instability drives the

gas towards the center, giving rise to a nuclear starburst and the formation of dense nuclear star clusters. Then, the active nucleus can be fueled by the evolution of the dense star cluster.

The gravitational instabilities of a galaxy disk are described in the next sections. Two-fluid instabilities are considered, and the critical role of gas is emphasized (section 6). Because of its dissipative character, the gas can cool down as soon as instabilities heat it, and maintain non-axisymmetric features like spiral structure. The corresponding gravity torques are the tool to transfer angular momentum. The most wide-spread instabilities are the $m = 2$ spirals and bars: their formation mechanisms, their family of orbits, their resonances, etc... are essential to better understand the dynamical gas fueling (section 4). It will be shown how bars can be destroyed, or re-born, how bars within bars develop, and how material could be driven towards the nucleus more efficiently through a hierarchy of bars.

Also very frequent are the $m = 1$ instabilities, lopsidedness and off-centring. Several possible mechanisms will be described for these instabilities, that can also favor material infall to the center (section 5). These include counter-rotation, warps or peculiar gaseous instabilities in a near-keplerian disk, a situation common in the neighborhood of central supermassive black holes.

Finally, external triggers through galaxy interactions and mergers should also be emphasized. Observational evidence of internal and external fueling will be discussed and compared. The role of gas and bars in minor and major mergers is investigated through numerical simulations. These external mechanisms are favored by hierarchical scenarios of galaxy formation, where massive galaxies are the result of the merging of several smaller entities. In this frame, it is expected that the central black hole mass increases in parallel to the mass of the galaxy, as observations seem to confirm.

One consequence of galaxy merging is the possibility of binary black hole formation. The evolution and history of the black hole population will be investigated through the main dynamical mechanisms (section 8), and implications on the fueling will be explored. The Starburst-AGN connection (competition or collaboration) is then described, in a cosmological perspective.

2 AGN fueling through dense nuclear star clusters

2.1 Fueling: why is there a problem?

To estimate more quantitatively the fueling problem, let us consider the typical luminosity and power of an active nucleus, that can be of the order or higher than 10^{46} erg/s. If we assume a mass-to-energy conversion efficiency $\epsilon \sim 10\%$ ($L = dM/dt c^2 \epsilon$), then the mass accretion rate dM/dt should be:

$$dM/dt \sim 1.7 (0.1/\epsilon) (L/10^{46} \text{ erg/s}) M_{\odot}/\text{yr}$$

If the duty cycle of the AGN is of the order of 10^8 yr, then a total mass up to $2 \cdot 10^8 M_{\odot}$ should be available. It is a significant fraction of the gas content of a typical galaxy, like the Milky Way! The time-scale to drive such a large mass to the center is likely to be larger than 1 Gyr.

For the mass to infall to the center, it must lose its angular momentum. Could this be due to viscous torques? In a geometrically thin accretion disk, one can consider the gas subsonic viscosity, where the viscous stress is modelled proportional (α) to the internal pressure, with a factor $\alpha < 1$. This can only gather in 1 Gyr the gas within 4α pc typically (e.g. Shlosman et al 1989, Phinney 1994). This shows that viscous torques will not couple the large-scale galaxy to the nucleus, only the very nuclear regions could play a role through viscous torques.

2.2 Are stars a possible fuel?

The stars themselves could provide gas to the nucleus, through their mass loss, if there is a local stellar cluster, dense and compact enough (core radius R_c of less than a pc, core mass M_{core} of the order of $10^8 M_{\odot}$). However, the mass loss rate derived from normal stellar evolution gives only $10^{-11} M_{\odot}/\text{yr}/M_{\odot}$, orders of magnitude below the required rate of a few M_{\odot}/yr . The contribution will be significant, only if a massive stellar cluster ($4 \cdot 10^9 M_{\odot}$) has just formed through a starburst (Norman & Scoville 1988). A coeval cluster can liberate $10^9 M_{\odot}$ on 10^8 yr, since mainly massive stars evolve together in the beginning. Thus the existence of a starburst in the first place solves also the problem of the AGN fueling, as in the symbiosis model of Williams et al (1999). The angular momentum problem is now reported to the starburst fueling, and could be solved only through large-scale dynamical processes.

There are several processes to fuel gas to the black hole, directly from the stars, and these could work for the low-luminosity end of AGNs; one can invoke:

- Bloated stars, a phenomenon that makes mass loss more efficient (Edwards 1980, Alexander & Netzer 1994, 1997),
- Tidal disruption of stars (Hills 1975, Frank & Rees 1976),

- Star Collisions (Spitzer & Saslaw 1966, Colgate 1967, Courvoisier et al 1996, Rauch 1999).

To quantify all these processes, it is important now to define the corresponding characteristic radii.

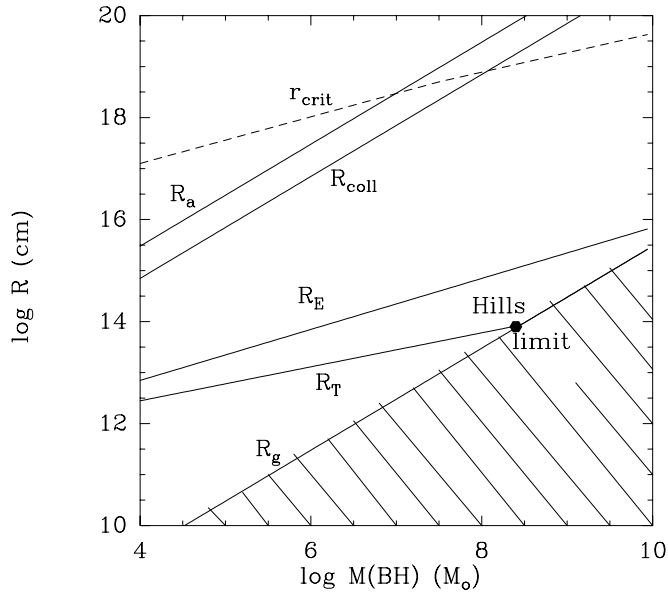


Figure 1. Characteristic radii, corresponding to the various physical phenomena, as a function of black hole mass: from top to bottom, R_a , the accretion radius, R_{coll} , the collision radius, R_E , the Eddington radius, R_T , the tidal radius, R_g , the gravitational radius (see text for definitions). Loss-cone effects are important inside the critical radius r_{crit} (see section 2.4).

2.3 Characteristic radii

First, it is obvious to define the “**accretion radius**” R_a , or the radius under which the black hole of mass M_\bullet dominates the dynamics, as a function of

the velocity dispersion of the stellar component around it V_∞ :

$$R_a = GM_\bullet/V_\infty^2 \sim 3 \times 10^{19} \text{ cm } M_8 (200/V_\infty)^2$$

where M_8 is the black hole mass in units of $10^8 M_\odot$. The radii are plotted in figure 1 (see also Frank & Rees 1976, Luminet 1987).

Then the “**collision radius**” R_{coll} , is the radius under which stellar collisions are disruptive, i.e. the freefall velocity around the black hole $(GM_\bullet/r)^{1/2}$ is comparable to the escape speed v_* of a typical individual star $(GM_*/r_*)^{1/2}$. For solar mass stars (escape velocity of the order of 500km/s):

$$R_{coll} \sim 7 \times 10^{18} \text{ cm } M_8$$

The “**Eddington radius**” is the radius under which a star receives more light than its Eddington luminosity:

$$R_E \sim R_*(M/M_*)^{1/2} \sim 7 \times 10^{14} \text{ cm } M_8^{1/2}$$

for solar mass stars. The radiation pressure can then disrupt the envelope, or at least form bloated stars, more fragile with respect to mass loss.

The “**tidal radius**” has a great importance, it is the radius under which a star is disrupted by the tidal forces of the black hole (calculated like a Roche radius):

$$R_T \sim R_*(M/M_*)^{1/3} \sim 6 \times 10^{13} \text{ cm } M_8^{1/3} \rho_*^{-1/3}$$

where ρ_* is the average density of solar mass stars. From that, we can estimate the accretion rate due to tidal disruption of stars, by integrating the mass available (in $\rho_{core} R_T^3$), divided by the dynamical time, in $\rho_{core}^{-1/2}$:

$$\text{DM/dt (tide)} \sim 0.3 M_\odot/\text{yr} (M_{core}/10^8 M_\odot)^{3/2} (0.01 \text{ pc}/R_c)^{9/2} M_8$$

Note that the efficiency of collisions between stars becomes larger than the tidal contribution, for large compactness of the nuclear star clusters, such as their velocity dispersion $\sigma_* > v_*$:

$$\text{DM/dt (coll)} \sim \text{DM/dt (tide)} (\sigma_*/v_*)^4$$

Finally, let us recall the horizon radius of the black hole (or “**gravitational radius**”) under which matter cannot escape:

$$R_g \sim 2GM_\bullet/c^2 \sim 310^{13} \text{ cm } M_8$$

As the black hole horizon grows faster with M_\bullet than the tidal radius, there is a limit, when $M_8 \sim 3$, above which the star disruption occurs inside the black hole, and there is no gaseous release or AGN activity (but the black hole grows even more rapidly). This is the Hills limit (Hills 1975).

2.4 Black hole growth by star accretion

Let us compute the time required to reach the critical mass M_c where $R_T = R_g$, above which stars are swallowed by the black hole without any gas radiation ($M_c = 3 \cdot 10^8 M_\odot$). When a tidal breakup of a star (of mass m , radius R) occurs, the energy required is taken from the orbital energy of the star

$$E_b = 3/4 G m^2/R$$

then the gas coming from the disruption will have an orbit of typical semi-major axis

$$r = (2M/3m)R/(1 - 2V^2R/3GM)$$

$$r = 1.5\text{pc } M_8 / (1 - \langle V^2 \rangle^{1/2} / 535\text{km/s})^2$$

For our own Galaxy, with a $2 \cdot 10^6 M_\odot$ black hole, this means a typical radius of the gas disk of 0.03 pc.

The black hole cannot swallow the gas too fast, the maximum rate occurs when it radiates at Eddington luminosity (above which the radiation pressure prevents the material to fall in). This maximum luminosity is: $L_E = 3.2 \cdot 10^4 (M/M_\odot) L_\odot$. For a mass M_c , the maximum is $10^{13} L_\odot$ (close to the peak luminosity of QSOs). Then the corresponding accretion rate, assuming an efficiency of $\epsilon = 10\text{-}20\%$ is $dM/dt_E = 1.1 \cdot 10^{-8} (M/M_\odot) M_\odot/\text{yr}$. This implies an exponential growth of the black hole; it takes only $1.6 \cdot 10^9$ yr to grow from a stellar black hole of $10 M_\odot$ to M_c :

$$t_E = 9.3 \cdot 10^7 \ln(M_c/M) \text{ yr}$$

Note that this very simple scheme would lead to a maximum at $z=2.8$ of the number of quasars. This maximum rate, however, is not realistic, since the black hole quickly gets short of fuel, as the neighbouring stars (in particular at low angular momentum) are depleted. Then it is necessary to consider a growth limited by stellar density ρ_s :

$$DM/dt = \rho_s \sigma V$$

where σ is the accretion cross-section, and V the typical stellar velocity. The corresponding time-scale to grow from M to M_c is

$$t_D = 1.7 \cdot 10^{15} \text{ yr } (\rho_s/M_\odot\text{pc}^{-3})^{-1} M/M_\odot^{-1/3} (1 - M/M_c^{1/3}) \langle V^2 \rangle^{1/2} \text{ (km/s)}$$

Typically in galaxy nuclei, $\rho_s = 10^7 M_\odot/\text{pc}^3$, $\langle V^2 \rangle^{1/2} = 225 \text{ km/s}$. A black hole could grow up to M_c in a Hubble time, and the luminosity at the end could be of the order of 10^{46} erg/s (see figure 2). More detailed considerations (Frank & Rees 1976, Lightman & Shapiro 1977) introduce the loss-cone effect: the angular momentum can diffuse faster than the energy (faster than a stellar relaxation time t_R). Stars with low angular momentum, or very eccentric

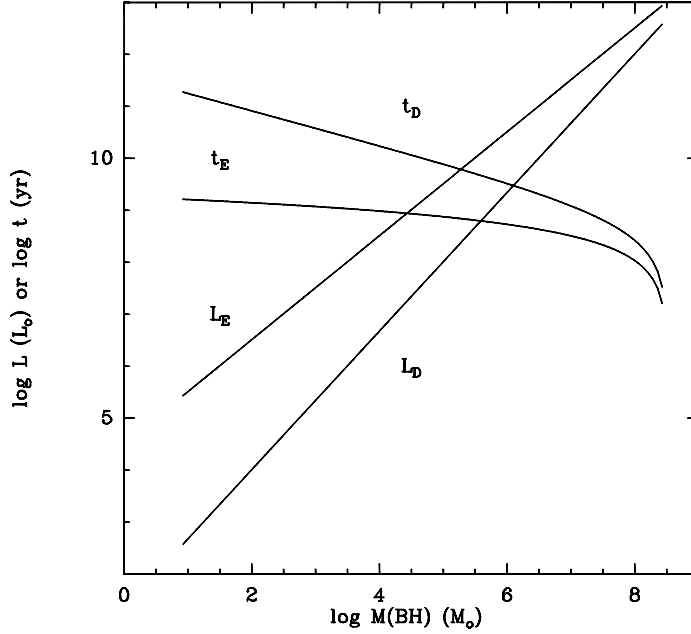


Figure 2. Growth of a supermassive black hole in two simple models: accretion at Eddington luminosity (time-scale t_E and corresponding luminosity L_E , as a function of black hole mass M_{BH}), and when accretion is limited by diffusion (t_D and L_D) (from Hills, 1975)

orbits, will be swallowed first. Since the low angular momentum stars are replenished faster, the loss-cone effect increases the accretion rate by: $t_l = t_R (1-e^2)$, with e the eccentricity of the orbits. This is significant inside a critical radius r_{crit} , where the loss-cone angle becomes larger than the diffusion angle $\theta_D \sim (t_{dyn}/t_R)^{1/2}$. This critical radius is also plotted in figure 1.

More detailed considerations also can change the above scenario, for instance when a mass spectrum for the stars is taken into account. The critical mass can be then be higher than M_c , because of large mass stars: giants are less dense and disrupted before solar-mass stars. This leads to higher luminosities for the active nuclei. Also the presence of the supermassive black hole may form a cusp of stars in the center. Then the stellar density is much higher and it is R_{coll} that limits the rate of accretion. Gas is produced by the star-star collisions, and again higher masses and luminosities can be reached.

2.5 Formation of a cusp of stars around the black hole

From a numerical resolution of the time-dependent Boltzmann equation, with the relevant diffusion coefficients, it can be shown that around a black hole at the center of a globular cluster, the stellar density should be of a power-law shape, with a slope of 7/4 (Bahcall & Wolf 1976). The relevant two-body relaxation time t_R is dependent on the number of bodies N in the system, as $t_R/t_c = N/\log N$, where t_c is the crossing time $= r_c/V$. For a galactic center, with a volumic density of stars of $10^7 M_\odot/\text{pc}^3$, this relaxation time is $3 \cdot 10^8$ yr.

The distribution of stars around a black hole can be described, according to the distance to the center:

- first for the stars not bound to the black hole, at $r > R_a$, their velocity distribution is Maxwellian, and their density profile has the isothermal power law in r^{-2} . There are also unbound stars inside R_a , but with a density in $r^{-1/2}$. This allows to compute the penetration rate of these unbound stars in the tidal or collision radius, to estimate the accretion rate. With a core stellar mass of $M_{core} = 10^7 - 3 \cdot 10^8 M_\odot$, a density 10^7 pc^{-3} , the accretion rate is, by tidal disruption:

$$dM/dt_{tide} = 1 M_\odot/\text{yr} M_8^{4/3}$$

and by stellar collisions:

$$dM/dt_{coll} = 0.1 M_\odot/\text{yr} M_8^3$$

- the orbits bound to the black hole $r < R_a$: due to the cusp, their density is in $r^{-7/4}$, there is an excess of stars inside R_{coll} , that favors stellar collisions.

More refined Monte-Carlo simulations with a distribution function $f(E, L, t)$, taking into account the velocity anisotropy, the disparition of disrupted stars, etc.. show that the stellar cluster cannot fuel the black hole indefinitely (Duncan & Shapiro 1983). The growth rate of the black hole and its luminosity decreases as $1/\text{time}$. The loss-cone theory and the simulations are in agreement: the accretion rate due to tidal disruptions is M_{core}/t_R , typically of $10^{-2} M_\odot/\text{yr}$, with a maximum lower than $1 M_\odot/\text{yr}$; this cannot explain the luminosity of QSOs. QSOs might be explained only when stellar collisions are included, the corresponding accretion rate is typically a hundred times higher.

Triaxial deviations from spherical symmetry of only 5% (due to a bar or binary black hole) can repopulate the loss-cone, increasing tidal disruption to QSOs levels. However, $t_{coll} < t_R$, and collisions may destroy the cusp (Norman & Silk 1983).

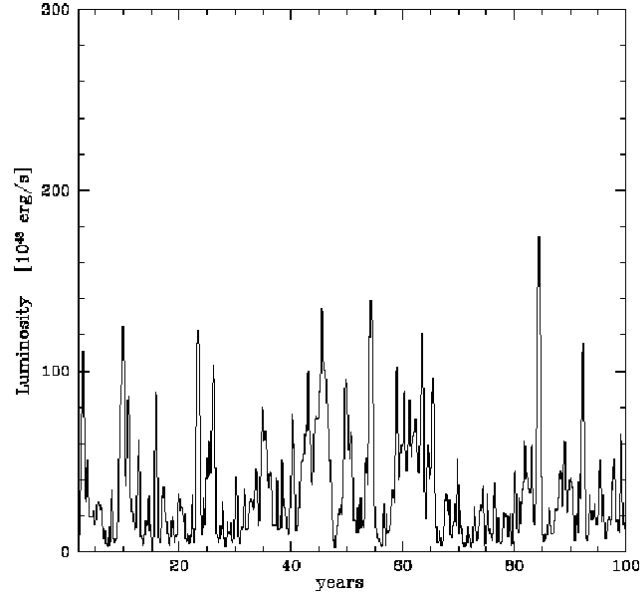


Figure 3. Light curve produced by the energy released in star collisions, with a collision rate of $\tau = 12$ collisions per yr, provided for instance by a star cluster of mass $10^7 M_{\odot}$, a core radius of $R_c = 0.001$ pc, surrounding a black hole of mass $10^9 M_{\odot}$ (from Torricelli-Campioni et al 2000).

2.6 Stellar Collisions

There is a tight analogy between the tidal disruption of stars by the black hole and the disruption of two stars during a head-on collision. The factor $\beta = v_{coll}/v_*$ ($v_* = 500\text{km/s}$ for a solar mass star) regulates the fate of collisions, and is equivalent to the factor of penetration of the star inside the tidal radius R_T/r_{peri} , where r_{peri} is the pericenter of the stellar orbit.

- if $\beta = 1$, the collision occurs near the collision radius R_{coll} , there is coalescence of the two stars; the result may quickly explodes as a supernova.
- if $\beta > 1$ a fraction of the mass is lost, and fuels the black hole.
- if $\beta \gg 1$ (well inside R_{coll}), a deformation in pancakes occurs, very similar to the tidal disruption, when $R_T/r_{peri} \gg 1$. Gas and debris are bound to the black hole.

Stellar collisions help to refill the loss-cone, although they flatten the stellar cusp (Rauch 1999). The collisions rate is comparable to the diffusion rate, that refill the central core.

It is now generally accepted that for low density nuclei, stellar evolution and tidal disruption is the main mechanism to bring matter to the black hole, and for high density nuclei, stellar collisions dominate the gas fueling. The evolution of the stellar density through these processes is then opposite, and accentuates the differences: – for $n < 10^7/\text{pc}^3$ the core then expands, due to heating that results from the settling of a small population of stars into orbits tightly bound to the black hole; – for $n > 10^7/\text{pc}^3$, the core shrinks due to the removal of kinetic energy by collisions. To give an order of magnitude, the nuclear density in our own Galaxy is estimated at $10^8 M_\odot/\text{pc}^3$ (Eckart et al 1993).

These mechanisms produce differing power-law slopes in the resulting stellar density cusp surrounding the black hole, $-7/4$ and $-1/2$ for low- and high-density nuclei, respectively (Murphy et al 1991, Rauch 1999). In simulations however (Rauch 1999), collisions tend to produce a flat core, instead of $r^{-1/2}$ law in Fokker-Planck studies, which imply isotropy (and are unable to treat sparse regions).

Finally, stellar collisions could explain both the high luminosities (up to 10^{45} ergs/s, Spitzer & Saslaw 1966, Colgate 1967), and the variability of some QSOs ($\sim 10\text{yr}$ scale) according to Courvoisier et al (1996), see figure 3.

But still, even with collisions, the most active quasars requiring $100 M_\odot/\text{yr}$ remain to be fueled. May be the gas from stars disruption can be stored in a disk, and suddenly poured in a burst of activity ? (Shields & Wheeler 1978). There might be tight relations with nuclear starbursts (Norman & Scoville 1988, Perry 1992, Williams et al 1999).

3 Large-scale instabilities

Since the available fuel near the black hole is not sufficient, and a large fraction of the gaseous mass of the galaxy disk must be involved, it is necessary to rely on violent large-scale instabilities, that can drive the matter inwards in a few dynamical times.

3.1 Gravitational stability

The conditions of stability of a dissipation-less component like the stellar one, is relatively well known. High enough velocity dispersions are required to suppress axisymmetric instabilities and even spirals, bars or z-instabilities. The

latter provide heating to the medium which becomes un-responsive. The gas is dissipative and has a completely different behaviour; it is always unstable, and its velocity dispersion is fixed by regulation and feed-back.

The local stability criterion has been established by Toomre (1964): stabilisation is obtained through pressure gradients (velocity dispersion c) at small scale, smaller than the Jeans length: $\lambda = ct_{ff} = c^2/G\Sigma$, where Σ is the disk surface density. At large scale, the rotation stabilises through centrifugal forces, more precisely the scales larger than $L_{crit} = 4\pi^2 G\Sigma/\kappa^2$ (where κ is the epicyclic frequency). The Safronov-Toomre criterion is obtained in equalling λ and L_{crit} :

$$Q = \frac{\kappa c}{3.36G\Sigma} > 1$$

For one component, a radial mode (ω, k) in a linear analysis obeys the dispersion relation (where k is the wave number):

$$\omega^2 = \kappa^2 + k^2 c^2 - 2\pi G\Sigma k = \kappa^2 + 4\pi^2 c^2/\lambda^2 - 4\pi^2 G\Sigma/\lambda$$

which means that self-gravity reduces the local frequency κ . If a stability criterium is easy to derive for one component, the same is not true for a two-components fluid, since the coupling between the two makes the ensemble more unstable than each one alone. The one-component criterion can be applied separately to the stellar and gas components, where the corresponding values of Σ and c are used, leading to Q_s and Q_g . Because $c_g \ll c_s$ however, only a small percentage of mass in gas can destabilize the whole disk, even when $Q_s > 1$ and $Q_g > 1$. For two fluids with gravitational coupling, the dispersion relation yields a criterion of neutral stability $\omega^2 = 0$:

$$\frac{2\pi Gk\Sigma_s}{\kappa^2 + k^2 c_s^2} + \frac{2\pi Gk\Sigma_g}{\kappa^2 + k^2 c_g^2} = F = 1$$

which gives directly an idea of the relative weight of gas and stars in the instabilities (cf Jog 1996). At low k (long waves), essentially the stars contribute to the instability, while at high k (short waves), the gas dominates. The neutral equilibrium requires the simultaneous solution of $d\omega^2(k)/dk = 0$, which leads to a system of 2 polynomial equations 4th and 3rd order in k , and no analytic criterion can be derived; there are only numerical solutions in terms of a two-fluid Q_{s-g} value, which is always lower than the Q_s or Q_g values. $Q_{s-g} = 1$ defines the neutral stability, by analogy with the one-fluid treatment, at the fastest growing λ $F = 2/(1 + Q_{s-g}^2)$. The stability depends strongly on the gas mass fraction ϵ (between 5 and 25%), and there can be sharp transitions from high to low values of λ , as the mass fraction increases from $\epsilon = 0.1$ to 0.15 for instance. When Q_s is high and Q_g is low (a frequent

situation, given the dissipation and cooling in the gas), the main instability is at small-scales. A gas-rich galaxy (with $\epsilon > 0.25$) is only stable at very low surface densities (this explains the Malin 1-type galaxies, Impey & Bothun 1989); the center of early-type galaxies, where Q_s is high, and Q_g is low (due to low gas velocity dispersion), could be dominated by the gas wavelength, even at very low gas mass fraction: this can explain spiral arms in galaxies such as NGC 2841 (Block et al 1996). Also interaction of galaxies, by bringing in a high amount of gas, may change abruptly the fastest growing wavelength from λ_s to λ_g , and trigger star-formation. Even beyond the neutral stability criterium, when $Q_{s-g} > 1$, a galaxy disk can be unstable with respect to non-axisymmetric perturbations, such as bars or spirals; in this case also, the two-fluid coupling increases the instability, i.e. the disk will form a bar, even if the stars or the gas alone are stable with respect to such perturbations (Jog 1992).

3.2 Feedback on the dynamics

Many photometric and kinematic studies have computed the Q values over galactic disks, and it appears that Q does not follow big variations, but on the contrary is almost constant over the systems, as if self-regulating processes were at work. The stellar dispersion has been studied in our own galaxy and in a few external galaxies by Lewis & Freeman (1989) and Bottema (1993). The velocity dispersion decreases exponentially with radius, in parallel to the stellar surface density, and Q_s is nearly constant as a function of radius, at least for large galaxies, and vary between 2 and 3 from galaxy to galaxy.

If the stellar disk can be considered as a self-gravitating infinite slab, locally isothermal (σ_z independent of z), its density obeys:

$$\rho = \rho_0 \operatorname{sech}^2(z/z_0) = \frac{\rho_0}{ch^2(z/z_0)}$$

where z_0 is the characteristic scale-height of the stellar disk, given by

$$z_0 = \frac{\sigma_z^2}{2\pi G \Sigma_s(r)}$$

where σ_z is the vertical velocity dispersion, and $\Sigma_s(r) = z_0 \rho_0$ is the surface density. The latter has a general exponential behaviour (e.g. Freeman 1970), with a radial scale-length h . The scale-height z_0 has been observed to be independent of radius (van der Kruit & Searle 1981, 1982, de Grijs et al 1997), and there are only small departures from isothermality in z (van der Kruit 1988). Then, if the mass to light ratio is constant with radius for the whole stellar disk, and there is no or little dark matter within the optical disk,

we expect to find a velocity dispersion varying as $e^{-r/2h}$. This is exactly what is found, within the large uncertainties (Bottema 1993). Since some galaxies of the sample are edge-on and others face-on, the comparison requires to know the relation between z and r projection of the dispersion. In the solar neighbourhood, $\sigma_z = 0.6\sigma_r$, and this ratio is assumed to be valid in external galaxies too.

As for the gaseous component, the vertical velocity dispersion is constant with radius in the outer parts of galaxies, where the rotation curve is flat (Dickey et al 1990, Combes & Becquaert 1997): $c_g \approx 6\text{km/s}$. The behaviour of $\kappa \propto 1/r$ (for a flat rotation curve) is exactly parallel to the gas surface density $\Sigma_g \propto 1/r$ (e.g. Bosma 1981), and therefore $Q_g \propto c_g\kappa/\Sigma_g$ is constant with radius in the outer parts. This strongly suggests a regulation mechanism, that could maintain the values of Q about constant for both stars and gas.

The mechanism could be simply gravitational instabilities coupled with gas dissipation. When the medium is cool enough, so that the Q value is too low, gravitational instabilities quickly provide heating. The stellar component cannot cool down and keeps hot, although this is somewhat moderated by the gravitational action of the gas, and the young stars born in the cool component. The gas is even more sensitive to the heating, but it can dissipate its disordered motions. The key point is that cooling encourages dynamical instabilities, and therefore produces heating, which is how the regulation works (cf Bertin & Romeo 1988).

It is tempting to relate the gas stability criterium ($Q_g \sim 1$) to the threshold for star formation in galaxy disks (cf Kennicutt, 1989). However, things are certainly less simple, since the gas component does not form stars as soon as it is unstable and form clouds. In the outer parts of galaxies, the HI gas that extends much further than the last radius of star-formation, appears patchy, clumpy, and following some kind of spiral structure. The outer gas is unstable at any scale. This suggests that instabilities are present, at the origin of cloud formation, and are the regulator of the constant c_g and Q_g (Lin & Pringle 1987).

Note that there are several ways to maintain Q constant, and that the stars and gas have chosen two different ways: the stellar component keeps its scale-height constant, while its velocity dispersion is exponentially decreasing with radius; the gas keeps its velocity dispersion constant, while its scale-height increases steadily with radius (linearly, when the rotation curve is flat). This might be related to the different radial distribution. The gas does not display an exponential radial profile, may be due to continued infall or accretion.

4 Bars

Spiral waves, bars, and more generally non-axisymmetric features in the galaxy mass distribution and potential can produce torques and gas radial inflows towards the center. Bars are more long-lived and usually represent a stronger perturbation, and therefore are the privileged way to fuel the nucleus dynamically. Let us first describe the orbits and resonances in a barred potential, to better understand the existence and direction of the torques.

4.1 Orbits and resonances

First, let us recall the characteristics of orbits in an axisymmetric potential $\Phi(r)$ in the plane $z = 0$. A circular orbit has an angular velocity $\Omega^2 = \frac{1}{r} \frac{d\Phi}{dr}$. In linearizing the potential in the neighborhood of a circular orbit, the motion of any particle can be expressed in first order by an epicyclic oscillation, of frequency κ ,

$$\kappa^2 = \frac{d^2\Phi}{dr^2} + 3\Omega^2 = r \frac{d\Omega^2}{dr} + 4\Omega^2$$

The general orbit is therefore the combination of a circle and an epicycle, or a rosette, since there is no rational relation between the two periods.

The bar creates a bisymmetric gravitational potential, with a predominant Fourier component $m = 2$, which rotates in the galaxy with the pattern speed Ω_b . There is a region in the plane where the pattern speed is equal to the frequency of rotation Ω , and where particles do not make any revolution in the rotating frame. This is the resonance of corotation (cf fig 4).

In the rotating frame, the effective angular velocity of a particle is $\Omega' = \Omega - \Omega_b$. There exists then regions in the galaxy where $\Omega' = \kappa/m$, i. e. where the epicyclic orbits close themselves after m lobes. The corresponding stars are aligned with the perturbation and closely follow it; they interact with it always with the same sign, and resonate with it. These zones are the Lindblad resonances, sketched in Figure 4. According to the relative values of Ω and κ in a realistic disk galaxy, and because the bar is a bisymmetric perturbation, the most important resonances are those for $m = 2$.

Periodic orbits in the bar rotating frame are orbits that close on themselves after one or more turns. Periodic orbits are the building blocks which determine the stellar distribution function, since they define families of trapped orbits around them. Trapped orbits are non-periodic, but oscillate about one periodic orbit, with a similar shape. The various families are (Contopoulos & Grosbol 1989):

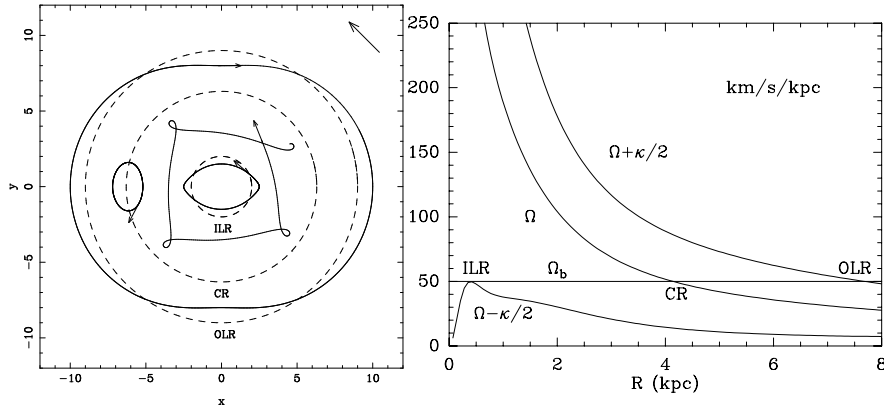


Figure 4. **left:** Various types of resonant orbits in a galaxy. At the ILR, the orbit is closed and elongated, and is direct in the rotating frame. At Corotation (CR), the orbit makes no turn, only an epicycle; at OLR, the orbit is closed, elongated and retrograde in the rotating frame. In between, the orbits are rosettes that do not close. **right:** Frequencies Ω , $\Omega - \kappa/2$ and $\Omega + \kappa/2$ in a galaxy disk. The bar pattern speed Ω_b is indicated, defining the locations of the Lindblad resonances.

- the x_1 family of periodic orbits is the main family supporting the bar. Orbits are elongated parallel to the bar, within corotation. They can look like simple ellipses, and with energy increasing, they can form a cusp, and even two loops at the extremities.
- the x_2 family exists only between the two inner Lindblad resonances (ILR), when they exist. They are more round, and elongated perpendicular to the bar. Even when there exist two ILRs in the axisymmetric sense, the existence of the x_2 family is not certain. When the bar is strong enough, the x_2 orbits disappear. The bar strength necessary to eliminate the x_2 family depends on the pattern speed Ω_b : the lower this speed, the stronger the bar must be.
- Outside corotation, the 2/1 orbits (which close after one turn and two epicycles) are run in the retrograde sense in the rotating frame; they are perpendicular to the bar inside the outer Lindblad resonance (OLR), and parallel to the bar slightly outside.

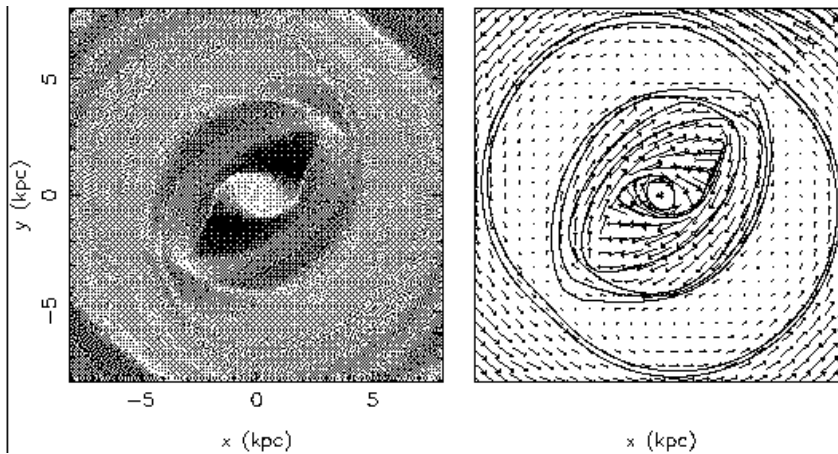


Figure 5. Response of the gas to a bar potential. The left panel shows the gas density in grey-scale and the right panel the gas flow lines and the velocity vectors in the rotating frame of the bar. The bar potential is at 45° from horizontal (from Athanassoula, 1992).

4.2 Gas flow in barred galaxies

In summary of the previous section, the orientation of the periodic orbits rotates by 90° at each resonance crossing, and they are successively parallel and perpendicular to the bar. The gas will first tend to follow these orbits, but the streamlines of gas cannot cross. Since periodic orbits do cross, gas clouds can encounter enhanced collisions, such that their orbits are changed. Instead of experiencing sudden 90° turns, their orbits will smoothly and gradually turn, following the schematic diagram of kinematic waves, first drawn by Kalnajs (1973), and illustrated in fig 8 and 9.

This interpretation predicts that the arms will be more wound when there exist more resonances; there will be a winding over 180° with only CR and OLR, with the gas aligned with the bar until corotation. When there exists 2 ILRs, the gas response can be perpendicular to the stellar bar. When there is barely one ILR, strong shocks can occur on the leading edge of the bar, corresponding to the offset dust lanes observed in barred galaxies (cf fig 5).

4.3 Angular momentum transfer

To minimize its total energy, a galaxy tends to concentrate its mass towards the center, and to transfer its angular momentum outwards (Lynden-Bell &

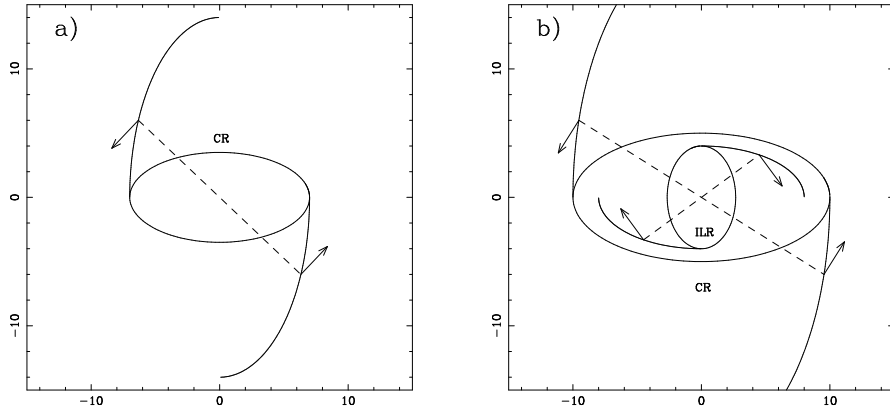


Figure 6. Schematic representation of the gravity torques exerted by the bar on the gaseous spiral: a) between CR and OLR, the gas acquires angular momentum and is driven outwards; b) between CR and ILR, the gas loses angular momentum (cf Combes 1988).

Kalnajs 1972). It is the role of the spiral structure to transport angular momentum from the center to the outer parts, and only trailing waves can do it. This transfer, mediated by non-axisymmetric instabilities, is the motor of secular evolution of galaxies, and of the formation of bars and resonant rings.

The angular momentum transfer is due to the torques exerted by the bar on the matter forming spiral arms. There is a phase shift between the density and the potential wells, resulting in torques schematized in fig 6. The gas is much more responsive to these torques, since they form the spirals in a barred galaxy. The torque changes sign at each resonance, where the spiral turns by 90° . Between the ILR and corotation, the torque is negative, while between CR and OLR, the torque is positive. These torques tend to depopulate the corotation region, and to accumulate gas towards the Lindblad resonances, in the shape of rings. Indeed, these rings then are aligned with the symmetry axis of the bar, and no net torque is acting on them. Numerical simulations of colliding gas clouds in a barred potential show that rings form in a few dynamical times, i.e. in a few Gyrs for the outer ring at OLR (Schwarz 1981), or in $\sim 10^8$ yr for nuclear rings at ILR (Combes & Gerin 1985).

This mechanism for ring formation has been confirmed by many studies, and confronted to observations, where it always encounters large success. The

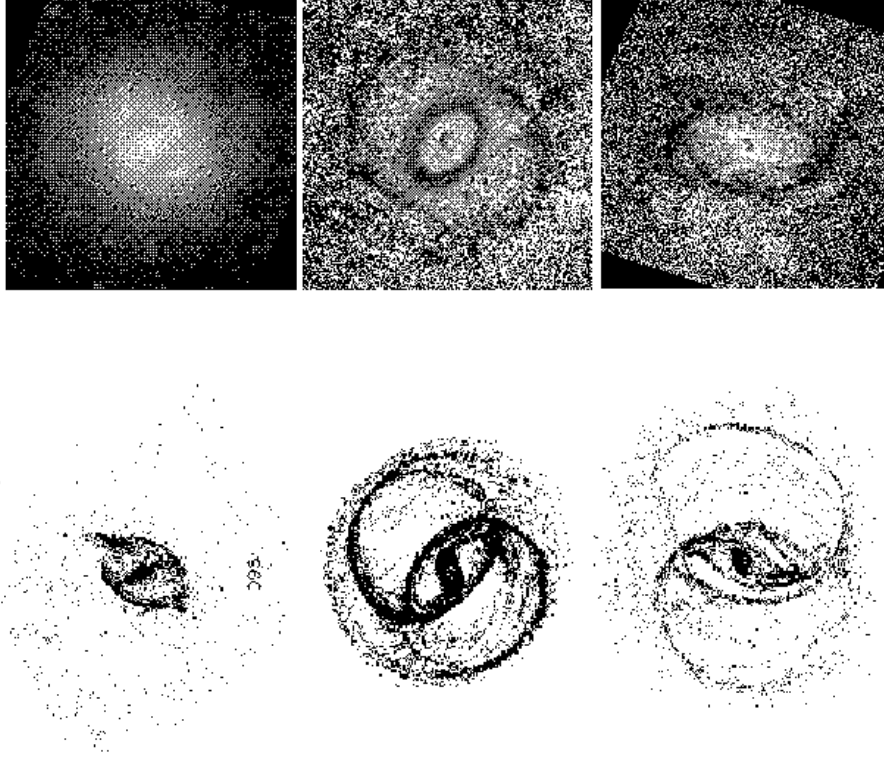


Figure 7. Comparison of observed maps (**top**) and corresponding simulations (**bottom**) for NGC 6300 (left), NGC 3081 (middle) and NGC 1433 (right). For NGC 3081 and NGC 1433, the top images are B-I colors (blue is dark), and for NGC 6300 it is the H-band image (from Buta & Combes 2000).

potential is obtained from photometry of the galaxies in NIR bands, and derived with a small number of assumptions (usually constant M/L over the disk). The simulation of the gas flow in the potential allow the derivation of the pattern speed (cf Buta & Combes 1996, and fig 7).

4.4 Fueling nuclear activity

The main problem to fuel the nucleus is to solve the transfer of angular momentum problem. Torques due to the bar are very efficient, but gas can be stalled in a nuclear ring at ILR. Other mechanisms can then be invoked: viscous torques, or dynamical friction of giant clouds (GMC) against stars. The viscosity is in general completely unefficient over the galactic disk, but the corresponding time-scale is decreasing with decreasing radius. Unfortunately, in the center of galaxies, the rotation is almost rigid, the shear is considerably reduced, and so are the viscous torques. The time-scale for dynamical friction becomes competitive below $r=100\text{pc}$ from the center (about $10^7 (r/100\text{pc})^2$ yr for a GMC of $10^7 M_\odot$). For the intermediate scales, a new mechanism is required.

Note that if there is a supermassive black hole in the nucleus, it is easier to bring the gas to the center. Indeed, the presence of a large mass can change the behaviour of the precession rate of orbits $\Omega - \kappa/2$: instead of increasing with radius inside ILR (as in fig 4), it will decrease.

Due to cloud collisions, the gas clouds lose energy, and their galactocentric distance shrinks. Since it tends to follow the periodic orbits, the gas streams in elliptical trajectories at lower and lower radii, with their major axes leading more and more the periodic orbit, since the precession rate (estimated by $\Omega - \kappa/2$ in the axisymmetric limit, for orbits near ILR, and by $\Omega + \kappa/2$ near OLR) increases with decreasing radii in most of the disk (fig 8). This regular shift forces the gas into a trailing spiral structure, from which the sense of the gravity torques can be easily derived. Inside corotation, the torques are negative, and the gas is driven inwards towards the inner Lindblad resonance (ILR). Inside ILR, and from the center, the precession rate is increasing with radius, so that the gas pattern due to collisions will be a leading spiral, instead of a trailing one (see Figure 9). The gravity torques are positive, which also contributes to the accumulation of gas at the ILR ring. This situation is only inverted in the case of a central mass concentration (for instance a black hole), for which the precession rate $\Omega - \kappa/2$ is monotonically increasing towards infinity with decreasing radii. Only then, the gravity torques will pull the gas towards the very center, and “fuel” the nucleus.

The problem reduces to forming the black hole in the first place. We show next that the accumulation of matter towards the center can produce a decoupling of a second bar inside the primary bar. This nuclear bar, and possibly other ones nested inside like russian dolls, can take over the action of gravity torques to drive the gas to the nucleus, as first proposed by Shlosman et al. (1989).

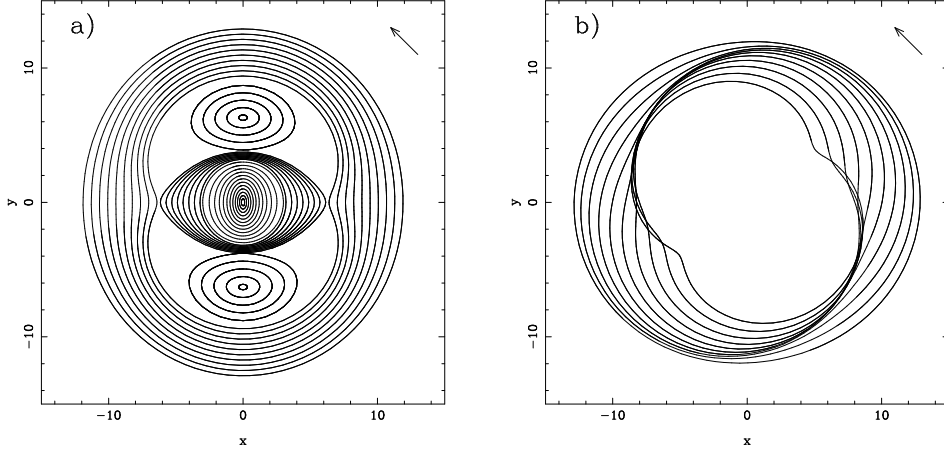


Figure 8. a) Periodic orbits in a barred galaxy ($\cos 2\theta$ potential, oriented horizontally). Their orientation rotates by $\pi/2$ at each resonance. b) The gas tends to follow these orbits, but is forced to precess more rapidly while losing energy and angular momentum, since $\Omega - \kappa/2$ is a decreasing function of radius.

4.5 Decoupling of a nuclear disk

The bar torques drive progressively more mass towards the center. This matter, gaseous at the beginning, forms stars, and gradually contributes to the formation of the bulge, since stars are elevated above the disk plane, through vertical resonances with the bar (e.g. Combes et al. 1990, Raha et al. 1991). When the mass accumulation is large enough, then the precessing rate $\Omega - \kappa/2$ curve is increasing strongly while the radius decreases, and this implies the formation of two inner Lindblad resonances. In between the two ILRs, the periodic orbits are perpendicular to the bar (x_2 orbits), and the bar loses its main supporters. The weakening of the primary bar, and the fact that the frequencies of the matter are considerably different now between the inner and outer disk, forces the decoupling of a nuclear disk, or nuclear bar from the large-scale bar (primary bar).

Nuclear disks are frequently observed, at many wavelengths: optical with the HST (e.g. Barth et al 1995, or fig 10) or in CO molecules with millimeter interferometers (Ishizuki et al 1990). A recent survey in the Virgo cluster (Rubin et al 1997) reveals that about 20% of the 80 spirals observed possess a decoupled nuclear disk. In nearly edge-on systems, these nuclear disks are

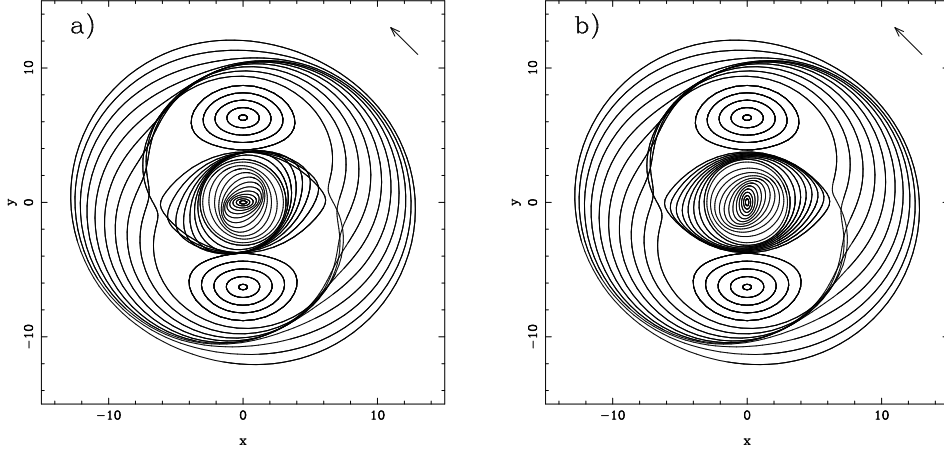


Figure 9. a) Without a central mass concentration, $\Omega - \kappa/2$ is increasing with radius in the center: the gas winds up in a leading spiral inside the ILR ring; b) with a central mass concentration, it is the reverse and the gas follows a trailing spiral structure, inside ILR.

conspicuous through large velocity gradients, like in the Milky-Way (Dame et al 1987) or NGC 891 (Garcia-Burillo & Guélin 1995).

4.6 Bars within bars

Secondary bars form through decoupling (Friedli & Martinet 1993, Combes 1994). The second bars rotate with a much faster angular velocity, and are observed with a random angle from the primary bar (see fig 11). To avoid chaos, the two bars have a resonance in common. It is frequent that the ILR of the primary coincides with the corotation of the secondary. Multiply periodic particle orbits have been identified in such time-varying potentials (Maciejewski & Sparke 1998). It is possible that the two bars exchange energy with each other, through non-linear coupling; then $m = 4$ and $m = 0$ modes are also expected, and these have been seen in simulations (Tagger et al. 1987, Masset & Tagger 1997). Even then, the life-time of the ensemble is rather short, a few rotations. But the nuclear bars could help to prolong the action of the primary bar towards the nucleus (as first proposed by Shlosman et al. 1989).

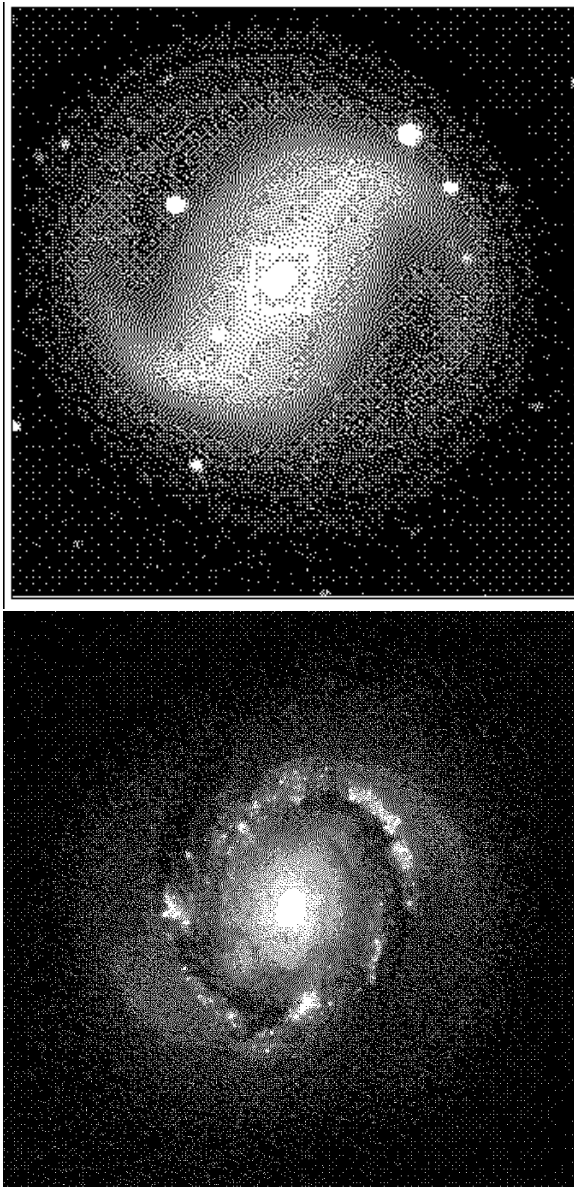


Figure 10. Photographs of the barred galaxy NGC 4314. **(top)** A general view of the bar and the spiral arms (photo from McDonald Observatory, Texas). **(bottom)** A zoom on the central parts (corresp. to the square in the first picture), with the Hubble Space Telescope. A nuclear ring can be discerned, within which a second independent spiral structure has developed (from Benedict et al. (1996).)

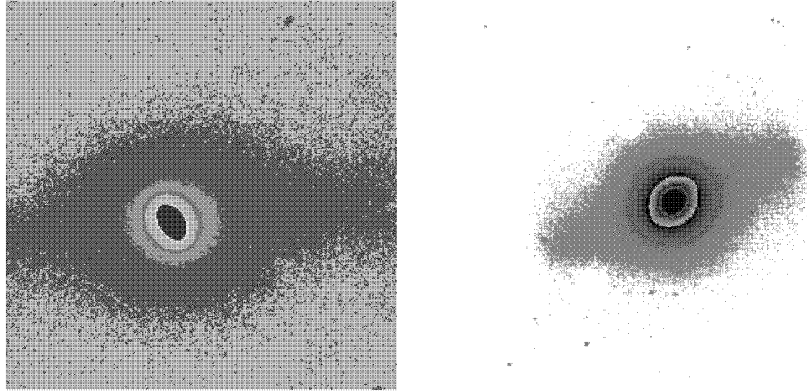


Figure 11. Examples of nuclear bars seen in the NIR bands: **left:** NGC 1433 in H; **right:** NGC 2217 in H; the field of view of both images is 2×2 arcmin, from Jungwiert et al (1997)

4.7 Bar destruction

The inflow of matter in the center can destroy the bar. It is sufficient that 5% of the mass of the disk has sunk inside the inner Lindblad resonance (Hasan & Norman 1990, Pfenniger & Norman 1990, Hasan et al 1993). But this depends on the mass distribution, on the size of the central concentration; a point mass like a black hole is more efficient (may be 2% is sufficient). The destruction is due to the mass re-organisation, that perturbs all the orbital structure: the x_1 orbits sustaining the bar for instance are shifted outwards. Near the center, the central mass axisymmetrizes the potential. Then there is a chaotic region, and outside a regular one again. When a central mass concentration exists initially, in N-body simulations, a bar still forms, but dissolves more quickly. It is also possible that after a bar has dissolved, another one forms, after sufficient gas accretion to generate new gravitational instabilities: the location of the resonances will not be the same.

4.8 Nuclear Spirals in Disk Galaxies

When the mass is concentrated towards the center in a galaxy, there can be several possibilities and mechanisms to fuel the nucleus: either bars within bars, as multi-mode stellar density waves, as described previously, or an unstable gas-dominated central disk (Heller & Shlosman 1994). Another possibility is simply a large-scale stellar bar, and a gaseous nuclear spiral by continu-

ity. It has been indeed proposed that the observed nuclear spirals are only gaseous (Elmegreen et al 1998, Regan & Mulchaey 1999). They could be acoustic waves, developing without self-gravity. Gas short waves are able to propagate inside ILR (and beyond OLR outside). The dispersion relation is (with v_s the sound speed):

$$m^2(\Omega - \Omega_p)^2 = \kappa^2 + k^2 v_s^2$$

for $m=2$

$$k^2 v_s^2 / 4 = (\Omega - \kappa/2 - \Omega_p)(\Omega + \kappa/2 - \Omega_p)$$

if $kR \gg 1$, the gas waves propagate only when $(\Omega - \kappa/2 > \Omega_p)$, in between two ILRs, or if there is only one ILR. Multi-arms (large m) are possible. The value of Q is large, since the gas is not self-gravitating. Simulations show the gas response in a stellar bar potential, and how the morphology depends on the sound speed and on the shape of the potential (Englmaier & Shlosman 2000, cf fig 12).

4.9 Bars in early- and late-types

Observations reveal that bars have different properties along the Hubble sequence (Elmegreen & Elmegreen 1985, 1989). In early-type galaxies, bars have flat profiles, while in late-types, they have exponential profiles. Also bars extend farther with respect to the disk exponential scale in late-types. Numerical simulations allow to interpret these features. Due to their relatively massive bulge, and large mass concentration, early-types have large precessing frequencies $\Omega - \kappa/2$ and tend to have large Ω_b (Combes & Elmegreen 1993). There exist then 2 ILRs, and bars end near their corotation. On the contrary, late-types have low $\Omega - \kappa/2$, and low Ω_b . Corotation is then far away in the disk, and lets the disk scale-length determine the bar length (see fig 13). The profile along the bar is therefore exponential, very similar to the disk profile. Early-types bars continuously grow in time, since angular momentum is transferred in outer regions. But late-types cannot, since there are not enough stars to accept angular momentum, and they stop to grow before. Since the existence of ILRs favors the radial gas inflows, the fueling appears more efficient in early-type galaxies.

4.10 Evolution along the Hubble sequence and growth of the black hole

Non-axisymmetric instabilities like bars force the galaxies to evolve towards large mass concentrations, large bulge-to-disk ratios, lower gas content through consumption by star formation. This means that a galaxy born as

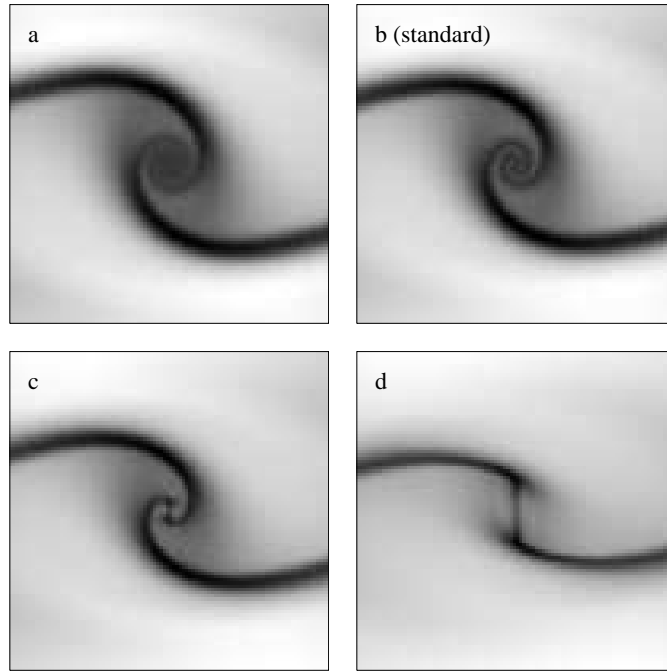


Figure 12. Gas streaming in a barred potential. The stellar bar is horizontal and extends more than twice the size of the box. The different morphologies are due only to the different values of the sound speed: (a) 7 km/s, (b) 10 km/s, (c) 14 km/s, (d) 20 km/s, from Englmaier & Shlosman (2000).

a late-type, will progressively evolve towards early-types, with a somewhat chaotic path, from barred to unbarred, and sometimes moving backwards, when the disk accretes mass. The gross lines of this evolution are sketched in fig 14.

To summarize this bar-driven evolution, and gather the main features obtained through N-body simulations, and supported by observations, it is interesting to test a toy model, in a semi-analytical way, including:

- star formation, with a combination of a quiescent rate, proportional to the gas density, in a time scale of 3 Gyr, and a bar-driven contribution, with a threshold ($Q < 1$) and a rate equal to $(1-Q)/t_*$, with t_* , the star-formation time-scale (proportional to the dynamical time-scale for gravitational instabilities).

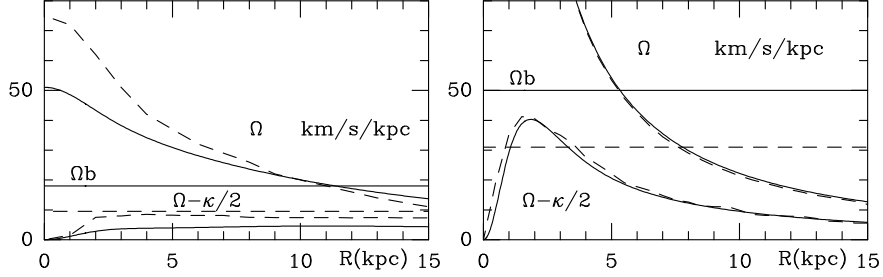


Figure 13. Rotation curves for late and early-type galaxy models, compared with the bar pattern speed. The initial values are full lines, while the final values are dashed lines. Left: late-type model; Right: early-type (from Combes & Elmegreen 1993).

- radial flows: when a bar is formed, gravity torques produce gas inflow, therefore with a threshold $Q < 1$ also, and rate $(1-Q)/t_{vis}$, with t_{vis} , the “gravitational viscosity” time-scale, $\sim \frac{1}{\Omega} \left(\frac{M_{tot}}{M_d} \right)^2$.
- bulge formation: the inflowing gas (and stars) are assumed to form the bulge through star-formation and vertical resonances
- death of bars: when $Q > 1$ (central concentrations, lack of gas and self-gravitating disk)
- gas infall: possibility of a continuous small infall or a periodically substantial one (from companions).
- black hole formation: a fixed fraction b_{eff} of the radial gas flow is taken to contribute to its formation, i.e. $dM_{bh}/dt = b_{eff} M_g (1-Q)/t_{vis}$, with a threshold $Q < 1$.

Figure 15 displays some results of the toy model (Combes, 2000). The most striking feature is the self-regulation of the stability parameter Q towards 1. Although the galaxy initially starts almost completely gaseous, the gas mass fraction soon stabilises to 10% of the total. Also the mass of the central concentration (or black hole) stabilises to a constant fraction of the bulge mass, as observed (Magorrian et al. 1998).

5 $m=1$ perturbations

Asymmetries, lopsidedness, one-arm spirals are also frequent in galactic disks, and may play a role in the fueling of the nucleus. Their physical processes are

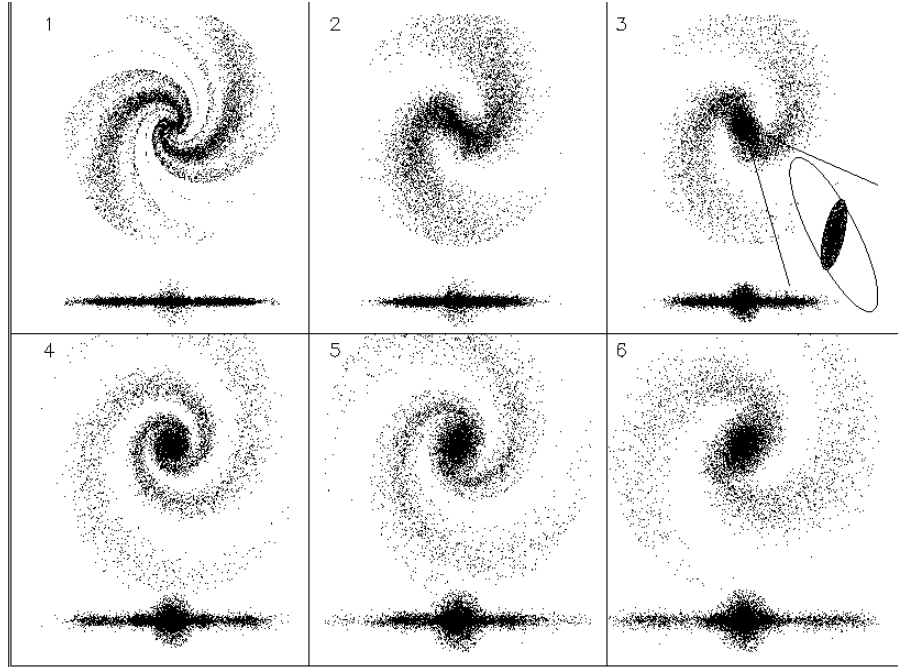


Figure 14. Cartoon of galaxy evolution along the Hubble sequence. A galaxy, with a small mass distributed mainly in a disk, without bulge (late-type), is unstable with respect to spiral and bar formation (steps 1 and 2). The bar drives the gas towards the center, and the bulge is building up (see in each frame the edge-on projection). When there is too much mass concentrated in the center, the bar is destroyed (step 4), and the gas coming from the outer parts, enrich the disk, and re-establish a larger disk to bulge ratio. Later on (steps 5 and 6), another bar will form, when the disk to bulge ratio is favorable. A secondary bar (cf step 3) may help the primary one to drive the mass towards the center. At the end, the galaxy may be classified early-type.

varied and different from the more familiar $m = 2$ instabilities, and these are first described briefly.

5.1 Physical nature of instabilities

The density wave theory has been developed in the WKBJ ($kr \gg 1$ approximation) and linear regime (e.g. Lin & Shu 1964, Toomre 1977). The amplification of the waves occurs at corotation, since the energy and angular

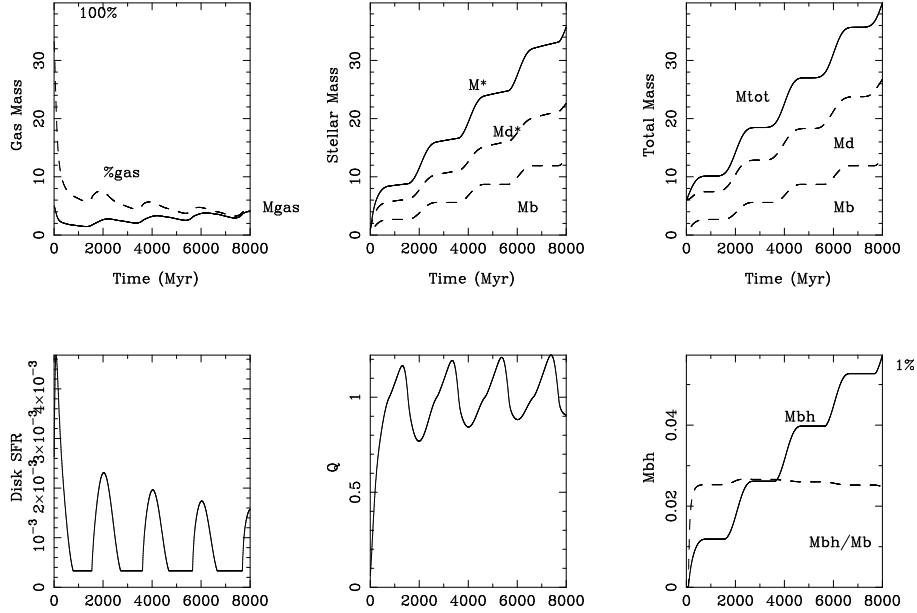


Figure 15. Model of periodic gas accretion in a galaxy with star formation, birth and death of bars, radial flows and black hole formation taken into account: **Top left** Full line: gas mass versus time; dash line: gas mass fraction. **Top middle** Full line: stellar mass; dash lines: disk stellar mass at top, and bottom bulge mass. **Top right** Full line: total mass; dash lines: total disk mass at top, and bottom bulge mass. **Bottom left** Disk star formation rate versus time. **Bottom middle** Toomre Q parameter. **Bottom right** Full line: mass of the central black hole, and dash line: mass ratio between the black hole and the bulge.

momentum of the perturbation are positive outside and negative inside corotation. Waves are partially transmitted, and partially reflected at corotation, which is a zone of evanescence for the waves if $Q > 1$. The wave transmitted will carry energy and angular momentum of opposite sign of the incident wave: for conservation, the reflected wave must have increased amplitude. Waves can spontaneously develop if the corotation amplifier is coupled to a reflection at a resonance or boundary (turning point). The feedback cycle may be the WASER (Mark 1974) or the SWING (Toomre 1977). The turning points are located at the radii when $\Omega_p = (\Omega \pm \kappa/m) (1-1/Q^2)^{1/2}$.

For $m = 1$ perturbations, there cannot exist ILR and OLR at the same

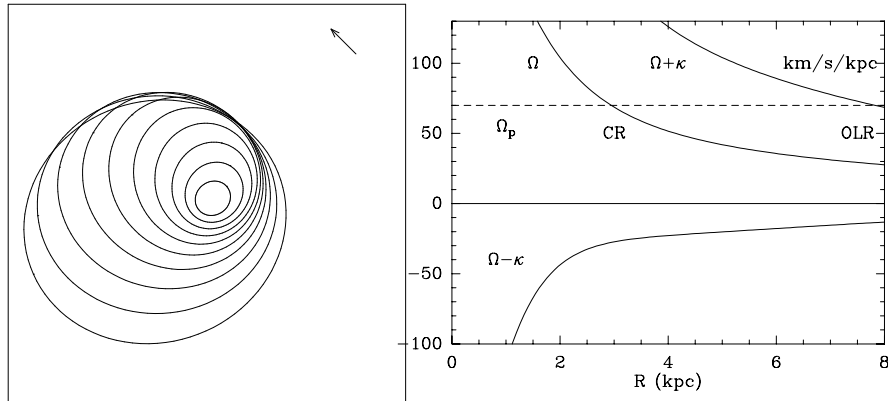


Figure 16. **left:** Pattern of lopsided ellipsoidal orbits forming a one-arm leading spiral. **right:** Frequencies Ω , $\Omega - \kappa$ and $\Omega + \kappa$ in a galaxy disk. A possible pattern speed Ω_p is indicated, allowing CR and OLR resonances

time (see fig 16). For lopsided instabilities, developing around a central mass in a nearly-keplerian disk, there exists another amplifier, which releases the need of corotation: the indirect potential, which is due to the off- centring of the central mass (Adams et al 1989, Shu et al 1990).

$$\Phi(r, \theta, t) = \alpha \omega^2 r \cos(\omega t - \theta)$$

This indirect potential creates in permanence a long-range force. The disk behaves like a resonant cavity with the off-centring constantly stimulating new long trailing waves. The central mass gains angular momentum, and the disk also outside corotation: this is not in contradiction, since in fact in a frame centered on the central mass, the angular momentum of the disk is of opposite sign (with respect to that centered on the system center of mass). While the growth rate of the mode γ must be $\sim \Omega$ for the SWING mechanism, here $\gamma \ll \Omega$. This mode allows the inner disk to lose angular momentum, and to inflow on the central mass.

5.2 Lopsidedness and $m = 1$ asymmetries

The $m = 1$ perturbation is present in most galactic disks (Richter & Sancisi 1994), often superposed to the $m = 2$ ones. These perturbations can be of different nature and origin, according to their scale (nuclear or extended disk), or whether they involve the gaseous or stellar disks.

Linear analysis, supported by numerical calculations, show that gaseous disks rotating around a central mass, are unstable for low value of the central mass (Heemskerk et al 1992). The instability disappears when the central mass equals the disk mass. For a gaseous disk, which can develop acoustic waves, and subject to the indirect term (or off-centering of the center of mass) as amplifier, an $m = 1$ can form and grow (Shu et al. 1990, Junqueira & Combes 1996).

For nuclear stellar disks, long lasting oscillations of a massive nucleus have been observed (Miller & Smith 1992, Tago & Iye 1998). For extended disks, off-centered in an extended dark halo, lopsidedness could survive, if the disk remains in the region of constant density (or constant $\Omega(r)$) of the halo (Levine & Sparke 1998).

In the special case of a stellar nuclear disk around a massive black-hole, it is possible that self-gravity is sufficient to compensate for the differential precession of the nearly keplerian orbits, and that a long-lasting $m = 1$ mode develops, or is maintained long after an external excitation (Bacon et al. 2000). This could be the explanation of the double nucleus observed for a long time in M31 (Bacon et al. 1994, Kormendy & Bender 1999), and for which an eccentric disk model has been proposed (Tremaine 1995, Statler 1999). In this $m = 1$ mode, the maximum density is obtained at the apocenter of the aligned elongated orbits. The pattern speed, equal to the orbital frequency of the barycentre of the stellar disk, is slow (3km/s/pc, fig 17), with respect to the orbital frequency of the stars themselves (250km/s/pc in the middle of the disk). The excitation of the $m = 1$ perturbation can then last more than 3000 rotation periods. This could be a frequent phenomenon around supermassive black-holes.

The decoupling of the nuclear disks also implies the possibility of decoupled z-oscillations, and it is frequent to observe these nuclear regions inclined at a different angle than the main disk. Jet orientations are not correlated with large-scale disk orientations in Seyfert Galaxies (Kinney et al. 2000), while they should be perpendicular to the accretion disk. As a well-studied example is the Galactic Center, our nearest supermassive black hole. There must be fueling in action. There is a large-scale bar, a nuclear bar/spiral, an $m = 1$ off-centring, a tilted disk (warped?) etc...

5.3 Counter-rotating components

The phenomenon of counter-rotating components is a tracer of galaxy interactions, mass accretion or mergers. It has been first discovered in ellipticals with kinematically decoupled cores (likely to be merger remnants, e.g. Barnes

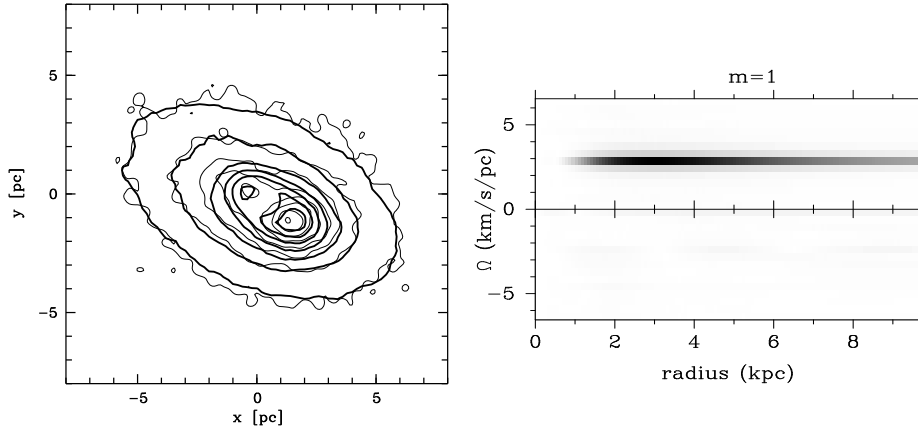


Figure 17. HST map in the visible of the nuclear disk surrounding the black hole of M31: thin lines are the observed contours, thick lines are those of the $m=1$ model simulations (**left**). Pattern speed as a function of radius, for the $m = 1$ mode obtained in the simulation (**right**), from Bacon et al (2000)

& Hernquist 1992). It has been observed also in many spirals; either two components of stars are counter-rotating, or the gas with respect to the stars, or even two components of gas, in different regions of the galaxies (Galletta 1987, Bertola et al 1992). In the special case of NGC 4550 (Rubin et al. 1992), two almost identical counter-rotating stellar disks are superposed along the line of sight.

These systems pose a number of questions, first from their formation scenario, but also about their stability, their life-time, etc.. Do special waves and instabilities develop in counter-rotating disks, and does this favor central gas accretion?

5.4 Stability

First, it appears that the counter-rotation (CR) can bring more stability. Even a small fraction of CR stars has a stabilising influence with respect to bar formation ($m = 2$), since the disk has then more velocity dispersion (Kalnajs 1977). But a one-arm instability is triggered, for a comparable quantities of CR and normal stars. This comes from the two-stream instability in flat disks, similar to that in CR plasmas (Lovelace et al. 1997). There develop

two $m = 1$ modes in the two components, with energies of opposite signs: the negative-E mode can grow by feeding energy in the positive-E mode.

A quasi-stationary one-arm structure forms, and lasts for about 1 to 5 periods (Comins et al. 1997). The structure is first leading, than trailing, and disappears. The formation of massive CR disks in spirals has been studied by Thakar & Ryden (1996, 1998).

5.5 Counter-rotation with gas

The presence of two streams of gas in the same plane will be very transient: strong shocks will occur, producing heating and rapid dissipation. The gas is then driven quickly to the center. But the two streams of gas could be in inclined planes, or at different radii. This is the case in polar rings, discovered in 0.5 % of all galaxies (Whitmore et al. 1990). After correction for selection effects (non optimal viewing, dimming, etc..) 5% of all S0 would have polar rings.

If there is only one gas stream, the problem is more similar to the two-stream instabilities of stellar disks mentioned above. However the gas is cooling, and is not easy to stabilise against $m = 2$ components. Both $m = 1$ and $m = 2$ may be present simultaneously in these systems. This is the case of the galaxy NGC 3593, composed of two CR stellar disks (Bertola et al 1996): in an extended stellar disk, is embedded a CR nuclear disk, possessing co-rotating gas. The molecular component associated with this nuclear disk reveals both a nuclear ring and a one-arm spiral structure outside of the ring (Garcia-Burillo et al. 2000). N-body simulations have shown that both structures can be explained by the superposition of $m = 1$ and $m = 2$ in the gas component, the ring being formed at the ILR of the bar (fig. 18). In the $m = 2$ pattern, two counter-rotating bars develop (fig 19).

6 Interactions and Mergers

Galaxy interactions can be the most efficient way to produce strong torques, and transfer the angular momentum away. During the interaction period, strong bars are triggered in the galaxy disks, and through the same mechanisms as described before, gas is driven inwards. During the merger, a complete change of geometry also brings most of the gas to the center. The main consequence is the trigger of spectacular starbursts, in particular in major mergers, i.e. merging about equal masses disk galaxies. The star forming activity is concentrated in nuclei, with some exceptions (as the antennae or Arp 299 for instance). The same gas inflow can also fuel an active nucleus,

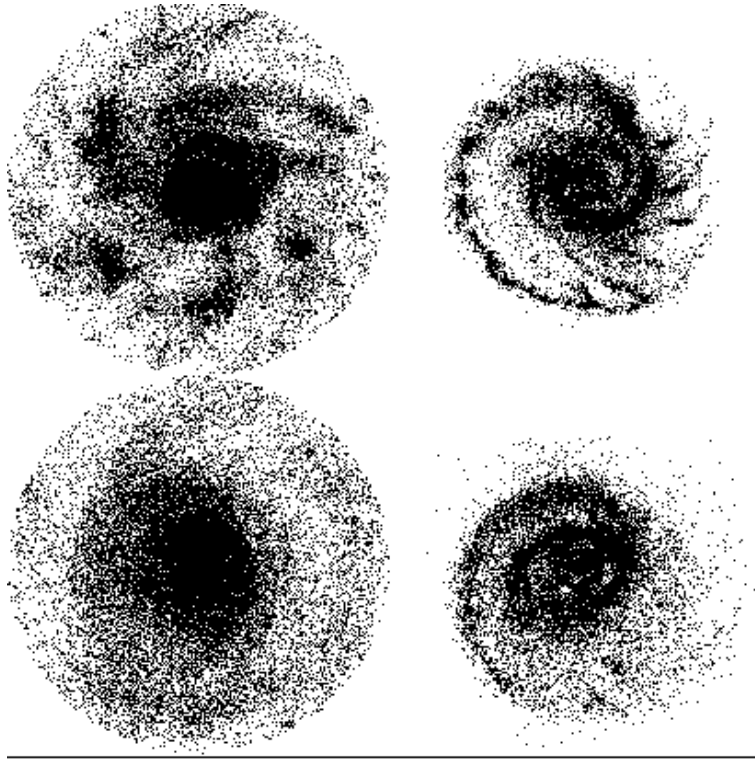


Figure 18. Particle plots of the stars (left) and the gas (right) for a model of the counter-rotating galaxy NGC3593, at successive epochs 200 and 400 Myr. Particles are plotted until a radius of 6.25 kpc. The majority of stars rotate in the direct sense, while the gas is retrograde (from Garcia-Burillo et al. 2000)

either directly, or indirectly through the coeval dense nuclear clusters formed in the starburst (cf section 2.2).

In these huge starbursts discovered by IRAS, CO concentrations suggest that the cause of the starburst is the concentration of huge gas masses in the center; the molecular gas represents a significant fraction of the dynamical mass (Scoville et al 1991). This gas must be brought to the center in a time-scale short enough with respect to the feedback time-scale of star-formation, i.e. a few 10^7 yrs (cf Larson 1987). This requires very strong gravity torques.

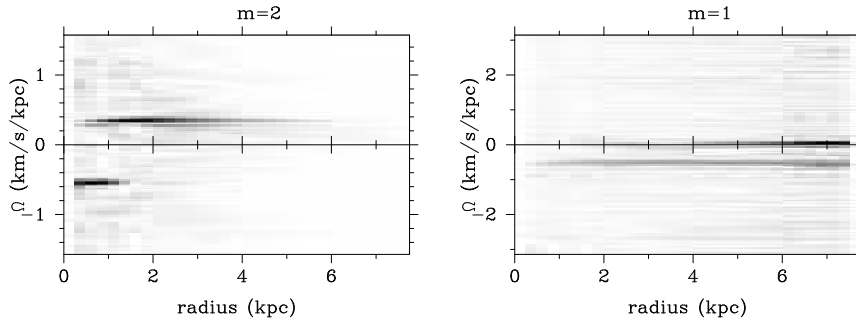


Figure 19. Pattern speed as a function of radius, in units of 100km/s/kpc , for the $m = 2$ mode, total density (**left**) and $m = 1$ mode, gas density (**right**), for the NGC3593 model of fig 18

. Note the presence of two counter-rotating bars.

6.1 Physical processes

Numerical simulations have enlightened the dynamical processes (Barnes & Hernquist 1992). They represent galaxies as 3-components systems, disks, bulges, and dark haloes. The latter play an important role, although they do not share most of the perturbations; they are essential to provide the dynamical friction that makes the baryonic systems decay and merge. It is the dark matter that takes most of the angular momentum away, allowing the luminous mass to fall towards the center (Barnes 1988).

Gas dissipation is also a key factor in merger simulations. The actual equivalent viscosity of the ISM is not well known, and it is not possible to reproduce the full multiphase medium. Two extreme modelisations are commonly used: the ISM is represented either as a continuous fluid, submitted to pressure forces, shock waves and artificial viscosity (finite difference scheme, SPH), or as colliding clouds, with no pressure forces and no shocks (sticky particles). Both can reproduce the main characteristics of gas flow in galaxies, provided that true viscous torques are negligible. The star-formation rate, global laws and corresponding feed-back are also not known in most perturbed dynamical situations, and present modelisations are rough approximations. Note that the star formation is itself fundamental for the dynamics, since it can lock the gas into the non-dissipative medium and halt for a while the mass transfer towards the center. Since stars are observed to be formed inside giant molecular clouds in our Galaxy, the latter being the result of agglomerations of smaller entities, one process could be to relate star forma-

tion to cloud-cloud collisions, in the sticky particles modelisation (Noguchi & Ishibashi 1986). Another more widely used is to adopt a Schmidt law for the SFR, i.e. the rate is proportional to a power n of the gas volumic density, n being between 1 and 2 (Mihos et al 1992). In both cases, it was shown that interacting galaxies were the site of strong starbursts, that could be explained both by the orbit crowding in density waves triggered by the tidal interactions, and by the gas inflow and central concentrations, accumulating the gas in small and very dense regions. This depends of course on the non-linearity of the Schmidt law, and SF-efficiency strongly depends on the power n (see e.g. Mihos et al 1992). Mihos & Hernquist (1994) use a hybrid-particles techniques, within SPH, to describe the effects of gas depletion and formation of a young star population.

Another peculiar feature of merging galaxies is the ability of forming giant complexes, that will soon become dense stellar clusters. This can be understood, given the larger velocity dispersion of perturbed systems. The disks are heated in tidal interactions, since the relative orbital energy is transformed into internal disordered motions. This has the consequence to increase the critical Jeans scale for gravitational instabilities, and to create giant complexes (e.g. Rand 1993). The global Jeans length is $\lambda \propto \sigma^2/\Sigma_g$, where σ is the velocity dispersion and Σ_g is the gas surface density of the galactic disk. The corresponding growth time is $\tau_{ff} \propto \sigma/\Sigma_g$, and the instabilities will occur as soon as $Q \propto \sigma\kappa/\Sigma_g$ becomes lower than 1. For the same ratio σ/Σ_g , a perturbed system with elevated σ and Σ_g will see the condensations of larger complexes of mass $M \propto \sigma^4/\Sigma_g$, in the same time-scale τ . These complexes with larger internal dispersions, and larger gravitational support will be less easy to disrupt through star-formation, which enhances the star-formation efficiency (Elmegreen et al 1993). The thermal Jeans length is also larger, due to the hotter gas temperature induced by the larger number of stars in the clouds, and high mass stars are favored. This explains the existence of giant and dense star clusters observed with HST in merging galaxies (Schweizer & Seitzer 1998, Meurer 1995). These clusters are estimated of masses $10^7 M_\odot$, and ages $3 \cdot 10^8$ yrs. They could evolve in typical globular clusters in about 15 Gyr.

6.2 Gas flow and starburst/AGN triggering

In major mergers, where the two interacting galaxies are of comparable mass, strong non-axisymmetric forces are exerted on the gas. But contrary to what could be expected, the main torques responsible for the gas inflow are not directly due to the companion. The tidal perturbations destabilise the pri-

mary disk, and the non-axisymmetric structures generated in the primary disk (bars, spirals) are responsible for the torques. The self-gravity of the primary disk, and its consequent gravitational instabilities, play the fundamental role. The internal structure therefore takes over from the tidal perturbations on the outer parts. The gas is provided by the primary disk itself. Again it is not the gas accreted from the companion which is the main trigger for activity, until the final merger of course. This is why the first parameter determining the characteristics of the merger event is the initial mass distribution in the two interacting galaxies (Mihos & Hernquist 1996). The mass ratio between the bulge and the disk is a more fundamental parameter than the geometry of the encounter (see fig 20 and 21).

The central bulge stabilises the disk with respect to external perturbations. If the bulge is sufficiently massive, the apparition of a strong bar is delayed until the final merging stages, and so is the gas inflow, and the consequent star-formation activity. But the starburst can then be stronger. When the primary disk is of very late type, without any bulge, the gravitational instability settles in as soon as the beginning of the interaction, there is then a continuous activity during the interaction, but at the end the starburst is less violent, since most of the gas has been progressively consumed before (see fig 22).

The effects of the geometry are more visible on the direct manifestations of the tidal interaction, i.e. on the tails and debris. For the galaxy experiencing a retrograde collision, no extended tidal tail is formed. There is no resonance effects in the target galaxy disk, and less violent material perturbations; a transient leading tidal arm is instead developed. There is however a tidally-induced two-arm density wave, and the subsequent torques produce gas inflow towards the center, as for the prograde encounter. During the interaction, it happens that the retrograde disk has more star formation than the prograde one, due to the larger gas content. For coplanar merger, the retrograde disk accretes a significant fraction of the gas from the prograde disk (Mihos & Hernquist 1996).

In the simulations, about 75% of the gas is consumed during the merger, whatever the internal structure of galaxies, or the geometry of the encounter (Mihos & Hernquist 1996). This is the most uncertain parameter, however. What is the fate of the rest of the gas? In general long tidal tails are entrained in the outer parts, especially in neutral hydrogen, since this is the most abundant component in external parts of galaxies. But most of the material of the tails is still bound to the system, and will rain down progressively onto the merger remnant (Hibbard 1995). Due to phase-wrapping process, it gives rise to shells and ripples. The HI fraction in the tails appear to increase as the

merger enters in more advanced stages. This might be due to the transformation of HI to H₂ in the central part. Also some of the gas is heated to the coronal phase (seen in X-rays).

During minor mergers, where the mass ratio between the two colliding galaxies is at least 3, the same features can be noticed: the first relevant parameter is the mass concentration in the galaxies before the interaction (Hernquist & Mihos 1995). The torques responsible for the gas mass inflow are exerted by the non-axisymmetric (essentially $m = 2$) potential developed in the disk. The torques are much stronger towards the center; the inflow time is of the order of the rotation time-scale at each radius.

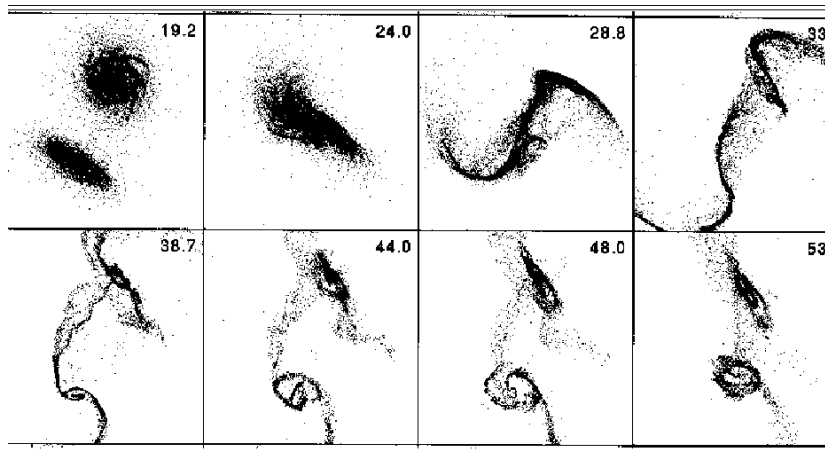


Figure 20. Simulations of the gas and young stellar components in the merger of disk/halo models. Time is indicated in units of 12 Myr (from Mihos & Hernquist 1996)

7 Observational evidence

The role of large-scale dynamics and interactions of galaxies is clear for the starburst activity in galaxies (Kennicutt et al 1987; Sanders et al 1988). IRAS ultra-luminous galaxies are all mergers (Sanders & Mirabel 1996), and the fraction of interacting galaxies is increasing with L_{IR}/L_B . But the influence of global dynamics is less clear for AGN activity. The fraction of Seyfert and quasars is however increasing with infrared luminosity, from 4 to 45% (Kim et al 1998).

A large fraction of galaxies with radio jets (FRII) are interacting (Heck-

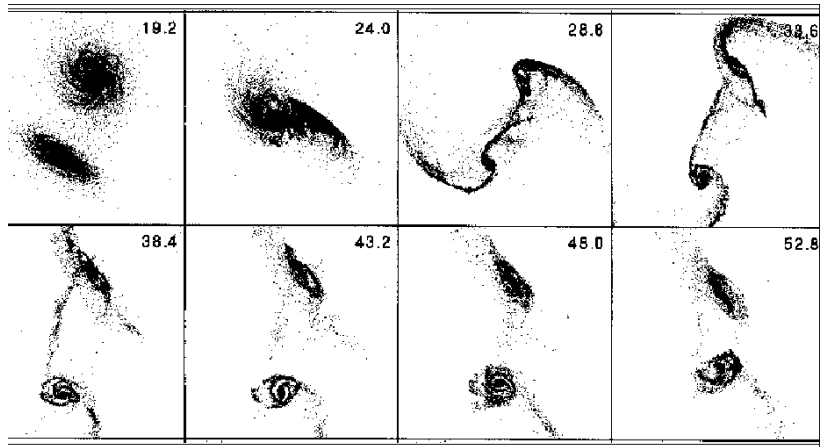


Figure 21. Same as fig 20 for the merger of disk/bulge/halo models

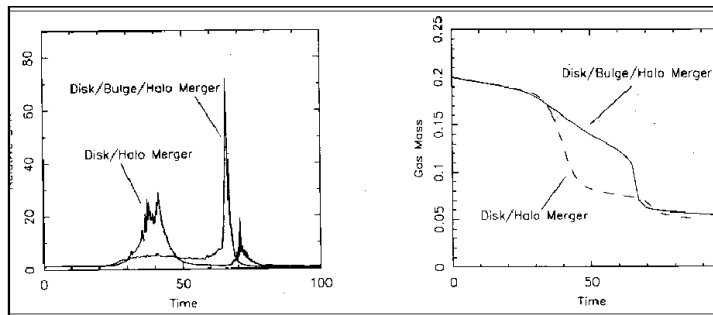


Figure 22. **left** Evolution of the global star formation rate (relative to isolated disks) for the two models of fig 20 and 21; **right** Evolution of the total gas mass

man et al 1986, Baum et al 1992). QSOs appear more than usual to interact with companions (Hutchings & Neff 1992; Hutchings & Morris 1995), and low-z quasars are mergers on HST images. Interactions are therefore efficient, but along years it has been very difficult to find any correlation between bars and nuclear activity. Are actually bars responsible for the fueling?

7.1 Search for correlations between bars and AGN

There have been several observational works revealing a correlation between nuclear activity and bars (Dahari 1984, Simkin et al 1980, Moles et al 1995). But the correlation is weak and depends on the definition of the samples, their completion and other subtle effects. Near-infrared images have often revealed bars in galaxies previously classified unbarred, certainly due to gas and dust effects. However, Seyfert galaxies observed in NIR do not statistically have more bars nor more interactions than a control sample (McLeod & Rieke 1995, Mulchaey & Regan 1997).

It is however evident from observations that bars are efficient to produce radial gas flows: barred galaxies have more H₂ gas concentration inside their central 500 pc than un-barred galaxies (cf Sakamoto et al 1999). Also, the radial flows level out abundance gradients in barred galaxies (Martin & Roy 1994).

Peletier et al (1999) and Knapen et al (2000) have recently re-visited the question, and took a lot of care with their active and control samples. Their Seyfert and control samples are different at 2.5σ , in the sense that Seyferts are more barred. They also measure the bar strength by the observed axial ratio in the images. In Seyferts, the fraction of strong bars is lower than in the control sample (Shlosman et al. 2000). Although a surprising result a priori, this is not unexpected, if bars are believed to be destroyed by central mass concentrations (cf section 4).

Regan & Mulchaey (1999) have studied 12 Seyfert galaxies with HST-NICMOS. Out of the 12, only 3 have nuclear bars but a majority show nuclear spirals. However their criterium for nuclear bars is that there exist leading dust lanes along this nuclear bar. This is not a required characteristic, since these secondary bars in general are not expected to have ILRs themselves.

A morphological study of the 891 galaxies in the Extended 12 μm Galaxy Sample (E12GS) has confirmed that Seyfert galaxies and LINERs have the same percentage of bars as normal spirals, contrary to HII/Starburst galaxies that have more bars (Hunt & Malkan 1999). However, active galaxies show rings significantly more often than normal galaxies or starbursts. The LINERs have more inner rings (by a factor 1.5), while Seyferts have more outer rings (by a factor 3-4) than normal galaxies. This might be due to the different time-scales for bar and ring formation: bars form relatively quickly, in a few 10^8 yr; they can drive matter to the central regions and trigger a starburst there, in the same time-scale. Outer rings form then, also under the gravity torques of the bar, but in the dynamical times of the outer regions, i.e. a few 10^9 yr. Since Seyferts are correlated with them, they would be associated to

delayed consequences of the starburst, or of the bar, which by this time begins to dissolve.

The percentage of AGN in the E12GS sample is 30%. As for interactions, 25% of the Seyferts are "peculiar" (disturbed), while 45% of the HII/Starbursts are. There is also a correlation between AGN and morphological types along the Hubble sequence. Seyferts tend to lie in early-types (Terlevich et al 1987, Moles et al 1995). This has to be related to the existence on inner Linblad resonances in early-types, favoring the fueling of the nucleus (e.g. section 4, Combes & Elmegreen 1993).

In summary, there might be some evidence of the role of large-scale dynamics on AGN fueling, but it is in general weak, except for the most powerful AGN. A good correlation between bars/interactions and AGN is not expected, from several arguments:

- there must be already a massive black hole in the nucleus, and this might be the case only for massive-bulge galaxies (not all barred galaxies)
- again a large central mass concentration (bulge) is necessary to produce an ILR and drive the gas inwards (early-types)
- other parameters, like geometrical parameters, control the fueling efficiency of interaction
- time-scales are not fitted: the AGN fueling is postponed after the interaction/bar episode
- there are other mechanisms to fuel AGN such that a dense nuclear cluster

7.2 *Galaxy interactions and nuclear activity*

Huge starbursts require galaxy interactions and mergers (e.g. Sanders & Mirabel 1996). For AGN of low luminosity, external triggering appears less necessary, since only $0.01 M_{\odot}/\text{yr}$ is required for a Seyfert like NGC 1068 for example, during 10^8 yr. However, once interactions drive gas to the nucleus, some activity must be revived. Time-scales may be the reason why the actions are not simultaneous. Large-scale gas has to be driven at very small scales in the center, and the whole process requires several intermediate steps.

Even for the good starburst/interactions correlations, there are exceptions for the low- luminosity samples. Interacting galaxies selected optically (not IRAS galaxies) are often not enhanced in star formation (Bushouse 1986, Lawrence et al 1989). Only the obviously merging galaxies, like the Toomre (1977) sample, are truly a starbursting class; it is difficult to reveal a progression along a possible evolutionary sequence (Heckman 1990). There are too many determining parameters: geometry, distance, gas content, etc...

A complication comes from the time-scales involved: the starburst phase is short, of the order of a few 10^8 yr, similar only to the end of the merging phase. It is more the presence of morphological distortions than the presence of nearby companions that is correlated with activity. More than 50% of ULIRGS possess multiple nuclei (Carico et al 1990, Graham et al 1990).

Are Seyfert galaxies preferentially interacting? According to Dahari (1984), 15% have close companions, compared to 3% in the control sample. But the Seyferts with or without companions have the same $H\alpha$ or radio power (Dahari 1985), although they may be more infrared bright with companions (Dahari & DeRobertis 1988, McKenty 1989). According to Keel et al (1985), there are 5% of Seyferts in control sample, and 25% in the close pairs of Arp Atlas. But it is possible that the Arp Atlas galaxies suffer from selection effects. Bushouse (1986) on the contrary finds a deficiency of Seyferts in interacting galaxies.

In summary, if the environment influence is evident for powerful QSOs, Radio-galaxies and BLacs, it is not so significant for Seyferts (deRobertis et al 1996).

Surprising observations also involve LSB (Low Surface Brightness Galaxies) that are about 6 times less bright than HSB. Their low evolution state is generally attributed to their isolated environment. A large fraction of active nuclei have been reported in their category: 65% in about 50 LSB instead of 1% expected for these low luminosities (Knezek & Schombert 1993, Sprayberry et al 1995). Are there unknown selection effects?

7.3 *Radio-galaxies*

Interactions are evident in the more powerful objects only. The FR-I objects have low-power, radio jets declining with distance, and are in general elliptical galaxies. Fewer than 10% show tails, and tidal interactions (Smith & Heckman 1989). The rarer FR-II objects, with high-power, are classical doubles (Cygnus A, Perseus A). They show a high percentage of interactions, from 32% (Yates et al 1989) to 100% (Hutchings 1987); most of them ($> 50\%$) have at least 2 companions, blue colors, star-forming regions (Heckman 1990, Gubanov 1991). Against the central radio-source, HI is seen in absorption, revealing that gas is most of the time infalling (absorption lines are blue-shifted, van Gorkom et al 1989).

Radio-loud QSO have 4-5 times more neighbors (Yee & Green 1984, Smith & Heckman 1990), while radio-quiet have 2 times more neighbors only with respect to a control sample. The morphology of QSO hosts is disturbed for 35-55% of them (Hutchings et al 1984, Smith et al 1986), while radio-loud

are perturbed at 70-80% (Smith et al 1986, Hutching 1987); this is confirmed with HST (Disney et al 1995).

The radio power of radio-galaxies has been related to the spin-down of a rotating supermassive black hole (Begelman 1986). The spin of the black hole may be acquired in galaxy interactions and mergers: either the black hole is spin up through gas accretion from an external disk, or through the merging of two black holes. In this respect, it is significant that radio-galaxies are generally giant ellipticals, since these are expected to be formed essentially by mergers.

7.4 Conclusion

Interactions are an essential mechanism in the fueling of QSOs, high-power radio-galaxies and ULIRGs. But they are not dominant in Seyferts and low-power radio-galaxies.

Observations reveal a close complicity between starbursts and AGN. AGN may be fueled by mass loss during PMS stellar evolution, of a coeval stellar cluster of $4 \cdot 10^9 M_{\odot}$, within 10pc (Norman & Scoville 1988). Within 10^8 yr, mass loss accumulates $1.5 \cdot 10^9 M_{\odot}$. Radiation (UV, X) from the inner accretion disk ionizes stellar envelopes, and form the BLR ($V \sim 3000$ km/s in the black hole potential well). The young stellar cluster requires a huge starburst, like those due to mergers. Shocks are then inevitable, model-independent supernovae can help transferring angular momentum. Starbursts and AGN are symbiotic systems (Collin et al 1988, Perry 1992, Williams et al 1999, Collin & Zahn 1999).

8 Black hole evolution

How are formed and grow the massive black holes in the center of galaxies? Can we explain the observed peak in quasar activity at $z = 2$ and the decline since then (see fig 23)? Why is this curve so parallel to the star formation history? If galaxies are themselves formed through interactions and mergers, what is the fate of the black holes in the merger, and are binary black holes observable ?

8.1 Black hole growth and activity life-time

It is widely believed that AGN derive their power from supermassive black holes, but their formation history, their demography, their activity time-scales are still debated. The two extreme hypotheses have been explored: either only

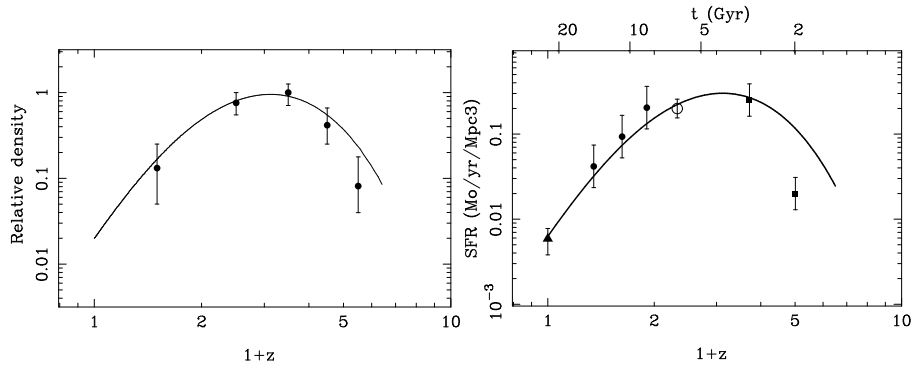


Figure 23. **left** Space density as a function of redshift, normalised to $z = 2 - 3$, for the Parkes flat-spectrum radio-loud quasars with $P_{11} > 7.2 \cdot 10^{26} \text{ W Hz}^{-1} \text{ sr}^{-1}$. The optically-selected quasars follow the same curve (from Shaver et al. 1996). **right** Cosmic history of star formation, for comparison. The various data points, coming from different surveys, give the universal metal ejection rate, or the star formation rate SFR (left-scale), as a function of redshift z .

a small percentage of galaxies become quasars, and they are continuously fueled, and active over Gyrs, or a massive black hole exists in almost every galaxy, but they have active periods of only a few 10^7 yr. In the first hypothesis, there should exist black holes with masses 100 times higher than the maximum observed today, and accretion rates much lower than the Eddington rate, and this is not supported (e.g. Cavaliere & Padovani 1989). Models with a duty cycle of $4 \cdot 10^7$ yr are favored, and many galaxies today should host a starving black hole (Haehnelt & Rees 1993).

The density of black holes derived today from the kinematics of galaxy centers at high spatial resolution (Magorrian et al. 1998, Ferrarese & Merritt 2000) strongly constrains the duty cycle time-scale. Also the cosmic background radiation detected at many wavelengths constrains the formation history. The volumic density of massive black holes today ρ_{bh} can be expressed as a function of the density of the bulges Ω_{bul} (normalized to the critical density to close the universe), and of the observed ratio between black-hole and bulge mass M_{bh}/M_{bul} :

$$\rho_{bh} = 1.1 \cdot 10^6 \frac{M_{bh}/M_{bul}}{0.002} \frac{\Omega_{bul}}{0.002 h^{-1}} M_{\odot} \text{ Mpc}^{-3}$$

with h the usual ratio of the Hubble constant to 100 km/s/Mpc (Haehnelt et al. 1998). It is interesting to note that this ratio largely exceeds (by a factor 10) the mass density in black holes needed to explain the blue light purely by

accretion on AGNs:

$$\rho_b = 1.4 \cdot 10^5 \frac{f_b \epsilon}{0.01} M_\odot \text{ Mpc}^{-3}$$

where f_b is the fraction of light emitted in blue, and ϵ the mass-to-energy conversion efficiency (section 2). This might be interpreted as a strong extinction of the blue light from AGNs, since part of the energy then can be seen in the infrared light. From the detected cosmic infrared radiation, and assuming that about 30% is coming from AGN (e.g. Genzel et al 1998), the predicted density is:

$$\rho_{ir} = 7.5 \cdot 10^5 \frac{f_{ir} \epsilon}{0.1} M_\odot \text{ Mpc}^{-3}$$

Part of the radiation is also observed through hard X-rays, and from the background hard-Xray radiation, the corresponding black hole density would be:

$$\rho_x = 3.8 \cdot 10^5 \frac{f_x \epsilon}{0.01} M_\odot \text{ Mpc}^{-3}$$

Note however that the sources contributing to the submillimetric and hard-Xray backgrounds are not the same, as discovered recently with Chandra (Severgnini et al. 2000). This could mean that even the hard-Xrays are extincted and most of the AGN radiation comes essentially in the infrared.

The best interpretation of the observations lead to an AGN activity lifetime of $\sim 4 \cdot 10^7$ yr. During this time the AGN would accrete and radiate at the Eddington limit. Before, the black hole is not massive enough to accrete efficiently, since the Eddington limit is proportional to its mass. The external fueling rate is larger than the limit during the growth phase, then during its bright phase of $\sim 4 \cdot 10^7$ yr the AGN radiates the most efficiently at Eddington luminosity, until the fuel is exhausted, and the AGN fades away (see fig 24).

In CDM hierarchical scenarios, the smallest halos form first, and they are denser, since the density of the Universe is a strong increasing function of redshift. Then the dynamical time-scale in such structures are much shorter. Due also to a higher gas mass fraction at high redshift (not yet consumed in stars), there are many reasons why the mass of the black holes formed are higher at high redshift (even if they form in smaller-mass systems). This can explain the density distribution and luminosity function observed for quasars (cf Boyle et al 1991): at high z , the quasars were both more numerous and their black holes more massive (assuming that we all see them in their bright phase, at Eddington luminosity).

To take into account these arguments, and reproduce the fact that the more massive black holes form in the smaller haloes, Haenelt & Rees (1993)

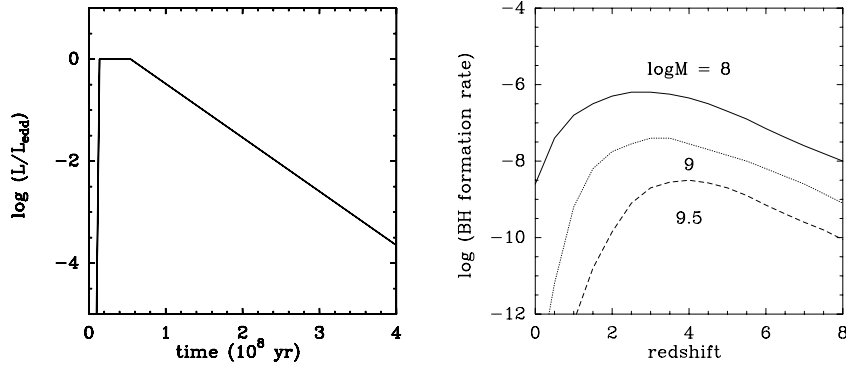


Figure 24. **left** A schematic view of the activity phase of a typical quasar: during the growth phase, the AGN does not radiate efficiently, although the fueling rate is larger than Eddington. After its luminous phase of $\sim 4 \cdot 10^7$ yr, the fuel is exhausted and the AGN fades away. **right** The black hole formation rate, or number density of newly formed BH per comoving volume, per time, and $\ln M$, in $\text{Mpc}^{-3} (10^7 \text{yr})^{-1} (\ln M)^{-1}$ (from Haehnelt & Rees 1993)

assume the ratio:

$$M_{bh}/M_{halo} \propto (1+z)^6 \exp(-v_*/v_{cir})^3$$

the dependence in $(1+z)$ corresponds to the higher efficiency to form a black hole at high z (due to the high densities), the exponential cut-off for low v_{cir} takes into account the difficulty of small mass system to retain gravitationally their gas in their small potential well (v_* is a normalizing value). With this model, the result is indeed that at low redshift, mostly small black holes are built, while the peak of formation of very massive black holes occurs at $z=4$ (see fig 24).

Today, merging of galaxies create a quasar in only small-mass gaseous objects. If the black hole formation process is not efficient at low redshift, the main process creating AGNs now is the tidally triggered nuclear activity, through gas accretion and minor mergers. To explain for instance the 1% of Seyferts in field galaxies (Huchra & Burg 1992), it is sufficient to assume a duty cycle of 1% of "normal" galaxies.

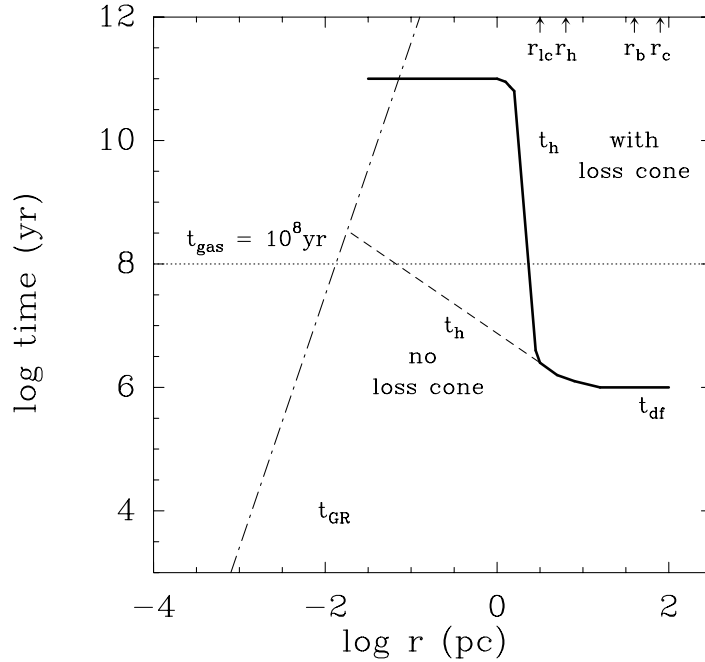


Figure 25. Time-scales relevant to the formation of a black-hole binary, in the merger remnant of two galaxies. Dynamical friction in the core of the elliptical galaxy formed, is acting in $t_{df} \sim 10^6$ yr. Within r_h , the evolution will proceed on $t_h = (r_h/r)t_{df}$ if loss-cone effects are neglected. However, taking into account depletion of stars in the loss cone leads to $t_h = 10^{11}$ yr, a much longer time. If infall of gas is considered, $t_{gas} \sim 10^8$ yr applies. At the end, gravitational radiation will take over (t_{GR}); from Begelman et al (1980). The core radius r_c , the “bound” radius r_b , the hardening radius r_h and the loss-cone radius r_{lc} are defined in the text.

8.2 Binary black hole formation

Given the large frequency of galaxy encounters and mergers, if there is a massive black hole in nearly every galaxy, the formation of a binary black hole should be a common phenomenon. The successive physical processes able to brake the two black holes in their relative orbit have been considered by Begelman et al (1980). Each black hole sinks first toward the merger remnant center through dynamical friction onto stars. A binary is formed; but the life-time of such a binary can be much larger than a Hubble time, if there is not enough stars to replenish the loss cone, where stars are able to

interact with the binary. Once a loss cone is created, it is replenished only through the 2-body relaxation between stars, and this can be very long (see section 2). Modelling the merger remnant as an elliptical, with a core of radius r_c and mass M_c (and corresponding velocity V_c), the radius where loss cone effects are significant is: $r_{lc}/r_c = (M_{bh}/M_c)^{3/4}$. The various time-scales involved, and corresponding characteristic scales are defined by the following steps:

- the dynamical friction on stars, in less than a galactic dynamical time,
$$t_{df} \sim (V_c/300\text{km/s})(r_c/100\text{pc})^2(10^8/M_{bh})\text{Myr}$$
- when the separation of the binary shrinks to a value $r_b = r_c(M_{bh}/M_c)^{1/3}$, the two black holes become bound together
- the binary hardens, with $r_h \propto (r/r_b)^{3/2}$
- but when $r < r_{lc} = (M_{bh}/M_c)^{3/4}r_c$, the stars available for the binary to interact with, are depleted through the loss cone effect, and replenished only by 2-body relaxation
- gas infall can reduce the binary life-time (whether the gas is flung out, or accreted, there is a contraction of the binary) in t_{gas}
- gravitational radiation shrinks the orbit on $t_{GR} \sim 0.3\text{Myr}(10^8/M_{bh})^3(r/0.003\text{pc})^4$ if the two black holes have comparable masses

All these time-scales are represented on figure 25. If the binary life-time is too long, another merger with another galaxy will bring a third black-hole. Since a three-body system is unstable, one of the three black-holes will be ejected by the gravitational slingshot effect.

Since the life-time of the binary is not short, there should be observable manifestations of massive black hole binaries. One of the best tracer is to detect the periodicity of the keplerian motion, with the period $P \sim 1.6\text{yr} r_{16}^{3/2} M_8^{-1/2}$. This is the case for the AGN OJ 287 where eclipses have been monitored for a century (Takalo 1994, Lehto & Valtonen 1996, Pietilä 1998). Also, if the black holes are rotating, and their spins have misaligned axes, they precess around the orbital one. Plasma beams (aligned to the hole axis) precess, and curved jets should be observed, with periods between 10^3 to 10^7 yr. This is frequently the case in radio structures observed with VLA and VLBI, modified by Doppler boosting, and light travel time (cf 3C 273, NGC 6251, 1928+738, Kaastra & Roos 1992; Roos et al 1993). Finally, pairs of radio

galaxies have been observed during their merger with four radio jets (3C75, Owen et al 1985).

Numerical simulations have brought more precision in the determination of the life-time of the binary, although numerical artifacts have given rise to debates. Ebisuzaki et al (1991) claimed that the life-time of the binary should be much shorter if its orbit is excentric, since then the binary can interact with more stars and release the loss cone problem. The first numerical simulations tended to show that orbit excentricity should grow quickly through dynamical friction (Fukushige et al 1992). Mikkola & Valtonen (1992) and others found that the excentricity in fact grows only very slowly.

Numerical simulations suffer from a restricted number of bodies N , and consequently of a large random velocity of the binary (that should decrease in $N^{-1/2}$). The binary then wanders in or even out of the loss cone, and the effect of the loss cone depletion does not occur (Makino et al 1993). Also the 2-body relaxation time is shorter than in the real system, contributing to replenish the cone. Numerically, the life-time of the binary depends on the total number of particles, i.e. the ratio between the black hole to particle mass:

$$t_b \propto (M_{bh}/m_*)^{0.3}.$$

To summarize the conclusions of several numerical computations, there is finally little dependence on excentricity e , only in rare cases, when e is large from the beginning (Quinlan 1996). Eventually, the wandering of the binary helps the merging of the two black holes (Quinlan & Hernquist 1997). The ejection out of the core of stars interacting with the binary weakens the stellar cusp, while the binary hardens. This may help to explain the surprisingly weak stellar cusps in the center of giant ellipticals observed recently with HST. Observations show that bright elliptical galaxies have weak cusps, while faint galaxies have strong cusps, with a power law slope of density versus radius of up to 2. A way to weaken the cusps is a sinking black hole (Nakano & Makino 1999), and this could be the case for giant galaxies that have experienced many mergers in their life.

8.3 Hierarchical merging scenario

Semi-analytic models, based on the Press-Schechter formalism, and a CDM hierarchical scenario of galaxy formation (Kauffmann & Haehnelt 2000), can reproduce rather well the essential observations: the proportionality relation between the bulge and black hole mass in every galaxy, the amount of energy radiated over the Hubble time due to accretion onto massive black holes, the

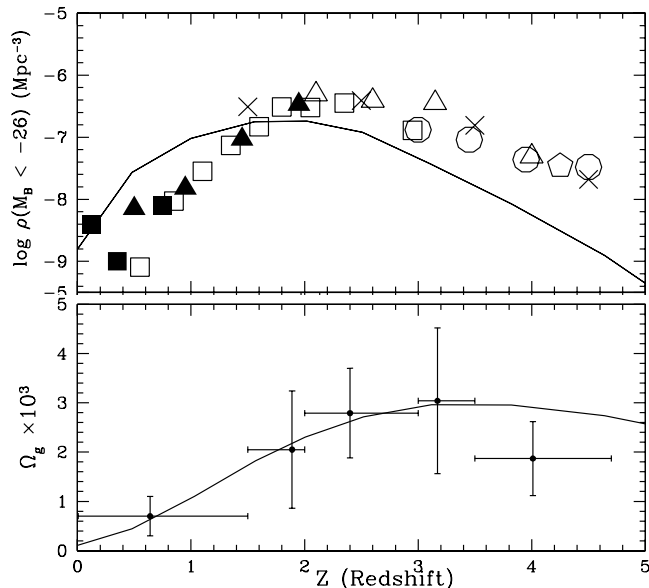


Figure 26. **top:** The evolution of the space density of quasars with $M_B < -26$ for the Λ CDM model (from Kauffmann & Haehnelt 2000). **bottom:** The cosmological mass density in cold gas in galaxies as a function of redshift for the Λ CDM model (from Kauffmann & Haehnelt 2000). The data is taken from Storrie-Lombardi et al. (1996).

past evolution of AGN activity. The assumptions are that the black holes grow through galaxy merging, both because of the merger of the pre-existing black holes, and due to the infall of gas to the center in the merging, that can fuel the merged BH. It is also assumed that the cold gas in galaxies decrease with time; this implies that the fueling will also decrease with time, accounting for the observed decline of AGN activity. Finally, the gas accretion time-scale is proportional to the dynamical time-scale, which is shorter at high redshift. The quasars convert mass to energy at a fixed efficiency, and cannot radiate more than the Eddington limit.

The results of such simulations are a strong decrease of the gas fraction in galaxies, from 75% at $z=3$ to 10% at $z=0$, corresponding to the gas density decrease observed in the damped Lyman alpha systems (cf fig 26); this implies that the black holes in the smallest ellipticals that formed at high z are relatively more massive, since there was more gas at this epoch. Ellipticals

forming today have smaller black holes. Also the brightness of AGN for a given galaxy was relatively higher in the past. The rapid decline of quasars is then due to several causes:

- a decrease in the merging rate (which is also the cause of the decrease of the star forming rate)
- the decrease of the gas amount in galaxies
- the decrease of the accretion rate (the dynamical processes are slower)

In these kind of models, it is natural to expect a ratio of proportionality between bulge and black hole masses, since they both form from the same mechanisms, the hierarchical merging, and the corresponding dynamical gas concentration. It is interesting to note that the life-time of the quasar phase, a few 10^7 yr is then derived.

9 Conclusions

The source of fueling depends on the strength and luminosity of the AGN:

- for low luminosity AGN and Seyferts, only stars from a dense nuclear cluster are sufficient (through tidal distortions and stellar collisions),
- for high luminosity AGN and quasars, large accretion rates are required, which involve large-scale gravitational instabilities. Those drive gas towards the center that trigger big starbursts, and the coeval compact cluster just formed can provide the fuel through mass loss of young stars and supernovae. This gas must have been driven from the galactic disks, through internal gravitational instabilities (bars, spirals), more generally the consequence of interactions and mergers.

Galaxy disks are in general far from stationary equilibrium, most often subject to $m = 2$ and $m = 1$ instabilities. These non-axisymmetric instabilities produce gravity torques, that drive the gas inwards. When the mass concentration towards the center is large enough, a secondary bar can decouple and rotate with a higher pattern speed. Embedded bars or non-axisymmetric structures can take over the gas flow to fuel the nucleus. The fueling is therefore favored in early-type objects.

Interactions and mergers also produce bars and non-axisymmetric structures, that fuel the nucleus through their gravity torques. They first trigger huge starbursts in the merger center, that could afterwards fuel the AGN. Since internal instabilities, external trigger and hierarchical merging both produce the bulges and fuel the nucleus, it is natural to expect a proportionality ratio in their masses.

Acknowledgments

I am very grateful to the organisers for inviting me to give these lectures, in a very friendly and scientifically exciting ambiance.

References

1. Adams, F. C., Ruden, S. P., Shu, F. H.: 1989, ApJ 347, 959
2. Alexander T., Netzer N.: 1994, MNRAS 270, 781
3. Alexander T., Netzer N.: 1997, MNRAS 284, 967
4. Athanassoula, E.: 1992, MNRAS 259, 345
5. Bacon R., Emsellem E., Monnet, G., Nieto, J. L.: 1994, A&A 281, 691
6. Bacon R., Emsellem E., Combes F. et al.: 2000, A&A in press
7. Bahcall, J. N., Wolf, R. A.: 1976, ApJ 209, 214
8. Barnes J.E.: 1988, ApJ 331, 699
9. Barnes J.E., Hernquist L.: 1992, ARAA 30, 705
10. Barth A., Ho L. C., Filippenko, A. V., Sargent, W. L.: 1995, AJ 110, 1009
11. Baum, S. A., Heckman, T. M., van Breugel, W.: 1992, ApJ 389, 208
12. Begelman M.C., Blandford R.D., Rees M.J.: 1980, Nature 287, 307
13. Begelman M.C.: 1986, Nature 322, 614
14. Benedict, F. G., Smith, B. J., Kenney, J. D. P. (1996) AJ 111, 1861
15. Bertin G., Romeo A.:1988 A&A, 195, 105
16. Bertola F., Buson, L. M., Zeilinger, W. W.: 1992, ApJ 401, L79
17. Bertola, F., Cinzano, P., Corsini, E.M., et al.: 1996, ApJ, 458, L67
18. Block D., Elmegreen, B. G., Wainscoat, R. J.:1996, Nature 381, 674
19. Bosma A.: 1981, AJ 86, 1825
20. Bottema R.:1993, A&A, 275, 16
21. Boyle B.J., Jones L.R., Shanks T. et al.: 1991, in "The Space Density of Quasars", ASP Vol 21, p. 191
22. Bushouse, H. A.: 1986, AJ 91, 255
23. Buta R., Combes F.: 1996, Fundamental Cosmic Physics, 17, p. 95-282
24. Buta R., Combes, F. : 2000, in "Dynamics of Galaxies: From the Early Universe to the Present", ed. F. Combes, G.A. Mamon, & V. Charmandaris, ASP Vol. 197, p. 11
25. Carico, D. P., Graham, J. R., Matthews, K. et al.:1990, ApJ 349, L39
26. Cavaliere A., Padovani P.: 1989, ApJ 340, L5
27. Colgate S.A.: 1967, ApJ 150, 163
28. Collin S., Dyson, J. E., McDowell, J. C., Perry, J.: 1988, MNRAS 232, 539

29. Collin S., Zahn J-P.: 1999, A&A 344, 433
30. Combes, F., Gerin, M.: 1985, A&A 150, 327
31. Combes, F. : 1988, in “Galactic and Extragalactic Star Formation”, ed. R. E. Pudritz and M. Fich, Kluwer, p. 475
32. Combes, F., Debbasch, F., Friedli, D., and Pfenniger, D.: 1990, A&A 233, 82
33. Combes, F., Elmegreen, B. G.: 1993, A&A, 271, 391
34. Combes F.: 1994, in “Mass-transfer induced activity in galaxies” ed. I. Shlosman, Cambridge Univ. Press, p. 170
35. Combes, F., Becquaert, J.-F.: 1997, A&A 326, 554
36. Combes, F. : 2000, in “Dynamics of Galaxies: From the Early Universe to the Present”, ed. F. Combes, G.A. Mamon, & V. Charmandaris, ASP Vol. 197, p. 15
37. Comins, N. F., Lovelace, R. V. E., Zeltwanger, T., Shorey, P.: 1997, ApJ 484, L33
38. Contopoulos, G. and Grosbol, P.: 1989 A&A Rev. 1, 261
39. Courvoisier, T. J.-L., Paltani, S., Walter, R.:1996, A&A 308, L17
40. Dahari, O.: 1984, AJ 89, 966
41. Dahari, O.: 1985, AJ 90, 1772
42. Dahari, O., DeRobertis M.: 1988, ApJ 331, 727
43. Dame T.M., Ungerechts H., Cohen R.S. et al.: 1987 ApJ, 322, 706
44. de Grijs, R., Peletier, R. F., van der Kruit, P. C.:1997, A&A 327, 966
45. Derobertis, M., Hayhoe, K., Yee, H. K. C.: 1996 AAS 189 109.04
46. Dickey J.M., Hanson M.M., Helou G.: 1990 ApJ, 352, 522
47. Disney M. J., Boyce, P. J., Blades, J. C., et al.: 1995, Nature 376, 150
48. Duncan M.J., Shapiro S.L.: 1983, ApJ 268, 565
49. Ebisuzaki, T., Makino, J., Okumura, S. K.: 1991, Nature 354, 212
50. Eckart A., Genzel, R., Hofmann, R., Sams, B. J., Tacconi-Garman, L. E.:1993, ApJ 407, L77
51. Edwards A.C.: 1980, MNRAS 190, 757
52. Elmegreen, B. G., Elmegreen, D. M.: 1985, ApJ 288, 438
53. Elmegreen, B. G., Elmegreen, D. M.: 1989, ApJ 342, 677
54. Elmegreen B.G., Kaufman M., Thomasson M.:1993, ApJ, 412, 90
55. Elmegreen, B. G., Elmegreen, D. M., Brinks, E. et al.: 1998, ApJ 503, L119
56. Englmaier, P., Shlosman, I.: 2000, ApJ 528, 677
57. Ferrarese, L., Merritt, D.: 2000, ApJ 539, L9
58. Frank J., Rees M.J.: 1976, MNRAS 176, 633
59. Freeman K. C., 1970 ApJ 160, 811
60. Friedli, D., & Martinet, L. 1993, A&A, 277, 27

61. Fukushige, T., Ebisuzaki, T., Makino, J.: 1992, ApJ 396, L61
62. Galletta, G.: 1987, ApJ 318, 531
63. Garcia-Burillo S., Guélin M.: 1995, A&A, 299, 657
64. Garcia-Burillo S., Sempere M.J., Combes F., Hunt L.K., Neri R.: 2000, A&A, in press
65. Genzel, R., Lutz, D., Sturm, E. et al.: 1998, ApJ 498, 579
66. Graham, J. R., Carico, D. P., Matthews, K., Neugebauer, G., Soifer, B. T., Wilson, T. D.: 1990, ApJ 354, L5
67. Gubanov A.G.: 1991, Pis'ma v Astronomicheskii Zhurnal vol. 17, p. 684
68. Haehnelt M.G., Rees M.J.: 1993, MNRAS 263, 168
69. Haehnelt M.G., Natarajan P., Rees M.J.: 1998, MNRAS 300, 817
70. Hasan, H., & Norman, C.A. 1990, ApJ, 361, 69
71. Hasan H., Pfenniger D., Norman C: 1993, ApJ 409, 91
72. Heckman T.M., Smith E., Baum S. et al.: 1986, ApJ 311, 526
73. Heckman T.M.: 1990, in "Paired and Interacting Galaxies" International Astronomical Union Colloquium No. 124 p 359
74. Heemskerk, M. H. M., Papaloizou, J. C., Savonije, G.: 1992, A&A 260, 161
75. Heller C.H., Shlosman I.: 1994 ApJ, 424, 84
76. Hernquist, L., Mihos, J.C.: 1995, ApJ 448, 41
77. Hibbard J.E.: 1995 PhD thesis, Columbia University
78. Hills J.G.: 1975, Nature 254, 295
79. Huchra J., Burg R.: 1992, ApJ 393, 90
80. Hunt L.K., Malkan M.A.: 1999 ApJ 516, 660
81. Hutchings, J. B., Crampton D., Campbell B.: 19984, ApJ 280, 41
82. Hutchings, J. B.: 1987 ApJ 320, 522
83. Hutchings, J. B., Neff S. G.: 1992 AJ 104, 1
84. Hutchings, J. B., Morris, S. C.: 1995, AJ 109, 928
85. Impey C., Bothun G.: 1989, ApJ, 341, 89
86. Ishizuki S., Kawabe R., Ishiguro M. et al.: 1990 Nature, 344, 224
87. Jog C.: 1992, ApJ, 390, 378
88. Jog C.: 1996, MNRAS, 278, 209
89. Jungwiert B., Combes, F., Axon, D. J., 1997, A&AS 125, 479
90. Junqueira S., Combes, F.: 1996, A&A 312, 703
91. Kaastra J.S., Roos N.: 1992, A&A 254, 96
92. Kalnajs, A. J.: 1973, Proc. Astron. Soc. Australia 2, 174
93. Kalnajs, A.J.: 1977, ApJ 212, 637
94. Kauffmann, G., Haehnelt, M.: 2000, MNRAS 311, 576
95. Keel W.C., Kennicutt R.C., Hummel, E., van der Hulst J-M.: 1985,

- AJ 90, 708
96. Kennicutt R.C.: 1989 ApJ, 344, 685
 97. Kennicutt R.C., Roettiger, K. A., Keel, W. C., van der Hulst, J. M., Hummel, E.: 1987, AJ 93, 1011
 98. Kim, D.-C., Veilleux, S., Sanders, D. B.: 1998 ApJ 508, 627
 99. Kinney A.L., Schmitt H.R., Clarke C.J., Pringle J.E., Ulvestad J.S., Antonucci R.R.J: 2000, ApJ in press (astro-ph/0002131)
 100. Knapen, J. H., Shlosman, I., Peletier R.F.: 2000, ApJ 529, 93
 101. Knezek, P., Schombert, J.: 1993, AAS 183, 4612
 102. Kormendy J., Bender R.: 1999, ApJ 522, 772
 103. Larson R.B. (1987) in "Starbursts and galaxy evolution", ed. T.X. Thuan, T. Montmerle, J. T. T. Van, Ed. Frontières, p. 467
 104. Lawrence, A., Rowan-Robinson, M., Leech, K., Jones, D. H. P., Wall, J. V.: 1989, MNRAS 240, 329
 105. Lehto H.J., Valtonen M.J.: 1996, ApJ 460, 207
 106. Levine S.E., Sparke L.S.: 1998, ApJ 496, L13
 107. Lewis J.R., Freeman K.C.: 1989, AJ, 97, 139
 108. Lin C.C., Shu F.H.: 1964, ApJ 140, 646
 109. Lin D.N.C., Pringle J.E.: 1987, ApJ 320, L87
 110. Lighthman A.P., Shapiro S.L.: 1977, ApJ 211, 244
 111. Lovelace, R. V. E., Jore, K. P., Haynes, M. P.: 1997, ApJ 475, 83
 112. Luminet J-P.: 1987, in "L'Activité dans les Galaxies", Annales de Physique, vol 12, p. 23 (Les Editions de Physique)
 113. Lynden-Bell, D., Kalnajs, A.J.:1972, MNRAS, 157, 1
 114. Maciejewski, W., & Sparke L.S. 1997, ApJ, 484, L117
 115. Magorrian, J., Tremaine, S., Richstone, D., et al. 1998, AJ, 115, 2285
 116. Makino, J., Fukushige, T., Okumura, S. K., Ebisuzaki, T.: 1993, PASJ 45, 303
 117. Mark J.W-K.: 1974, ApJ 193, 539
 118. Martin P., Roy J-R.: 1994, ApJ 424, 599
 119. Masset F., Tagger M.: 1997, A&A 322, 442
 120. McKenty J.: 1989, ApJ 343, 125
 121. Mcleod, K. K., Rieke, G. H.: 1995, ApJ 441, 96
 122. Meurer G.R.: 1996, in "The interplay between massive star formation, the ISM and galaxy evolution", ed. D. Kunth, B. Guiderdoni, M. Heydari, T. X. Thuan, Editions Frontières, p. 333
 123. Mihos J.C., Hernquist L.:1994 ApJ, 437, 611
 124. Mihos, J.C., Hernquist, L.:1996, ApJ, 464, 641.
 125. Mihos J.C., Richstone D.O., Bothun G.D.:1992, ApJ, 400, 153
 126. Mikkola, S., Valtonen, M. J.: 1992, MNRAS 259, 115

127. Miller R.H., Smith B.F.: 1992, ApJ 393, 508
128. Moles, M., Marquez, I., Perez, E.: 1995, ApJ 438, 604
129. Mulchaey J.S., Regan M.W.: 1997, ApJ 482, L135
130. Murphy, B. W., Cohn, H. N., Durisen, R. H.: 1991, ApJ 370, 60
131. Nakano T., Makino J.: 1999 ApJ 525, 77
132. Noguchi M., Ishibashi S.:1986, MNRAS, 219, 305
133. Norman C., Silk J.: 1983, ApJ 266, 502
134. Norman C., Scoville N.Z.: 1988, ApJ 332, 124
135. Owen, F. N., Odea, C. P., Inoue, M., Eilek, J. A.:1985 ApJ 294, L85
136. Peletier, R. F., Knapen, J. H., Shlosman, I., et al.: 1999, ApJS 125, 363
137. Perry J.: 1992, in “Relationships between active galactic nuclei and starburst galaxies”, ed. A. V. Filippenko, ASP Conference Series (ASP: San Francisco), vol. 31, p. 169.
138. Pietilä H.: 1998, ApJ 508, 669
139. Pfenniger, D., & Norman, C. 1990, ApJ, 363, 391
140. Phinney E.S.: 1994, in “Mass-transfer induced activity in galaxies” ed. I. Shlosman, Cambridge Univ. Press, p. 1
141. Quinlan G.D.: 1996, New A. 1, 35
142. Quinlan G.D., Hernquist L.: 1997, New A. 2, 533
143. Raha, N., Sellwood, J. A., James, R. A., Kahn, F.: 1991, Nature 352, 411
144. Rand R.J.: 1993 ApJ 410, 68
145. Rauch K.P.: 1999, ApJ 514, 725
146. Regan, M. W., Mulchaey, J. S.: 1999 AJ 117, 2676
147. Richter O-G., Sancisi R.: 1994, A&A 290, L9
148. Roos N., Kaastra J.S., Hummel C.A.: 1993, ApJ 409, 130
149. Rubin V.C., Kenney J.D.P., Young J.S.:1997 AJ 113, 1250
150. Rubin, V. C., Graham, J. A., Kenney, J. D. P.: 1992, ApJ 394, L9
151. Sakamoto, K., Okumura, S. K., Ishizuki, S., Scoville, N. Z.: 1999, ApJ 525, 691
152. Sanders D.B., Mirabel I.F.: 1996, ARAA 34, 749
153. Sanders, D. B., Soifer, B. T., Elias, J. H., Neugebauer, G., Matthews, K.: 1988, ApJ 328, L35
154. Shaver, P. A., Wall, J. V., Kellermann, K. I., Jackson, C. A., Hawkins, M. R. S.: 1996, Nature 384, 439
155. Schwarz, M. P.: 1981, ApJ 247, 77
156. Schweizer, F., Seitzer, P.: 1998, AJ 116, 2206
157. Scoville N.Z., Sargent, A. I., Sanders, D. B., Soifer, B. T.: 1991, ApJ 366, L5

158. Severgnini, P., Maiolino, R., Salvati, M., et al.: 2000 A&A 360, 457
159. Shields G.A., Wheeler J.C.: 1978, ApJ 222, 667
160. Shlosman, I., Frank J., Begelman M.C.: 1989, Nature 338, 45
161. Shlosman, I., Peletier, R. F., Knapen, J. H. : 2000, ApJ 535, L83
162. Shu, F. H., Tremaine, S., Adams, F. C., Ruden, S. P.: 1990, ApJ 358, 495
163. Simkin S.M., Su H.J., Schwarz M.P.: 1980, ApJ, 237, 404
164. Smith E., Heckman T., Bothun G. et al.: 1986, ApJ 306, 64
165. Smith E., Heckman T.: 1989, ApJ 641, 358
166. Smith E., Heckman T.: 1990, ApJ 348, 38
167. Spitzer L., Saslaw W.C.: 1966, ApJ 143, 400
168. Sprayberry, D., Impey, C. D., Bothun, G. D., Irwin, M. J.: 1995, AJ 109, 558
169. Statler T.S.: 1999, ApJ 524, L87
170. Storrie-Lombardi, L.J., MacMahon, R.G., Irwin, M.J.: 1996, MNRAS, 283, L79
171. Taga M., Iye M.: 1998, MNRAS 299, 111
172. Tagger, M., Sygnet, J. F., Athanassoula, E., Pellat, R.: 1987, ApJ 318, L43
173. Takalo L.O.: 1994, Vistas Astron. 38,77
174. Terlevich, R., Melnick, J., Moles, M.: 1987, in "Observational Evidence of Activity in Galaxies", IAU 121, Kluwer Academic Publishers, Dordrecht, p.499
175. Thakar A.R., Ryden B.S.: 1996, ApJ 461, 55
176. Thakar A.R., Ryden B.S.: 1998, ApJ 506, 93
177. Toomre A.: 1964, ApJ, 139, 1217
178. Toomre A.: 1977, ARAA 15, 437
179. Torricelli-Ciamponi, G., Foellmi, C., Courvoisier, T. J.-L., Paltani, S.: 2000, A&A 358, 57
180. Tremaine S.: 1995, AJ 110, 628
181. van der Kruit P.C., Searle L.:1981 A&A, 95, 105
182. van der Kruit P.C., Searle L.:1982 A&A, 105, 351
183. van der Kruit P.C.: 1988 A&A, 192, 117
184. van Gorkom, J. H., Knapp, G. R., Ekers, R. D., et al.: 1989, AJ 97, 708
185. Whitmore, B. C., Lucas, R. A., McElroy, D. B., et al.: 1990 AJ 100, 1489
186. Williams R. J. R., Baker, A. C., Perry, J.J.: 1999, MNRAS 310, 913
187. Yates, M. G., Miller, L., Peacock, J. A.: 1989, MNRAS 240, 129
188. Yee H., Green R.: 1984, ApJ 280, 79